Nitrate dynamics in an agricultural watershed, Minnesota, U.S.A.

A THESIS SUBMITTED TO THE FACULTY OF THE
UNIVERSITY OF MINNESOTA
BY

KATHERINE MCLELLAN

IN PARTIAL FULFILLMENT OF THE REQUIREMENTS
FOR THE DEGREE OF
MASTER OF SCIENCE

Dr. Joe Magner, Advisor

May 2018

Copyright

Acknowledgements

I am grateful to my advisor, Dr. Joe Magner, for his support and guidance on this project. I am also thankful to my committee members, Dr. Diana Karwan, Dr. John Nieber, and Dr. Crystal Ng, for their time and insights on my research.

For additional research support and advice, I am indebted to Dr. Galin Jones, Dr. Andry Ranaivoson, Dr. Jeffrey Strock, Dr. Brandy Toner, Dr. Bruce Wilson, Scott Alexander, Emily Deering, and Lu Zhang.

For logistical support in the field and the lab, I am grateful to Eleanor Arpin, Derrick Ferguson, Hilary Pierce, Alex Van Kirk, and Travis Vieths. Special thanks to Eleanor Arpin for her extensive work on this project throughout the summer of 2017. Thank you to Elizabeth Lundstrom for analyzing cation and anion water samples and assistance in using results. I would also like to thank Tracy Fallon for help in navigating graduate program requirements and protocols. Additionally, I am grateful to my family and friends for their support during my time in graduate school.

This project was funded by a research grant from the U.S. Environmental Protection Agency (EPA) Clean Water Act Section 319 program.

Abstract

Nitrate is a common agricultural pollutant with severe ecological consequences. The Cottonwood River Watershed is an intensively managed agricultural setting within the Mississippi River Basin, which exports nitrate that contributes to the hypoxic zone in the Gulf of Mexico. Understanding nitrate sources, pathways, and processes within the Cottonwood River Watershed sheds light on the larger issue of nitrate loading to the Gulf. This study utilizes an end-member mixing analysis (EMMA) approach to identify water and nitrate sources to the Cottonwood River; performs a nitrate mass balance to find magnitudes of in-stream nitrate transformation over a range of discharges and dates; and assesses long-term concentration-discharge relationships in the watershed to elucidate nitrate processes. The three main sources of water that contribute to the Cottonwood River at Lamberton (approximately halfway up the watershed) are tile drainage, shallow groundwater, and Quaternary aquifer groundwater. In-stream nitrate removal is found to be highest at low discharge levels, which occur late in the crop growing season. Concentration-discharge relationships from long-term datasets confirm this finding, and demonstrate that intra-annual variation in nitrate concentrations has decreased during the period of record. Nitrate removal within the stream channel is attributed to biogeochemical processes such as denitrification and dissimilatory nitrate reduction to ammonium, which disproportionately decrease in-stream nitrate concentrations at low discharges. Given the low in-stream nitrate removal at high discharges, management of nitrate in agricultural watersheds should strive to decrease peak discharges.

Table of Contents

List of Figures

List of Tables

1. Introduction

1.1. Nitrogen cycle and anthropogenic impacts

Nitrogen is a naturally occurring element in terrestrial and aquatic ecosystems, and is often a limiting nutrient for biological productivity (Gruber and Galloway 2008; Delwiche 1970). The unreactive form of nitrogen, dinitrogen (N_2), is converted to reactive nitrogen by lightning and biological nitrogen fixation (Galloway et al. 2003; Delwiche 1970). In aquatic ecosystems, nitrogen can exist as nitrate (NO_3^-), nitrite (NO_2^-), ammonium (NH^{4+}), or as organic forms (Delwiche 1970). Nitrate is the focus of this study because of its relevance to biological productivity and water quality (Goolsby and Battaglin 2001; Rabalais, Turner, and Wiseman 2002). Humans have altered the nitrogen cycle significantly, principally by increasing the rate of conversion of dinitrogen to reactive nitrogen species (Galloway et al. 2003). This impacts the atmosphere, terrestrial system, groundwater, inland surface water, and the oceans (Galloway et al. 2003). This study will focus on impacts of nitrate to riverine systems.

Three anthropogenic mechanisms increase the production of reactive nitrogen, and by extension of nitrate. First, the Haber-Bosch process allows humans to convert reactive nitrogen to ammonia (NH_3), most of which is used to produce agricultural fertilizer (Galloway et al. 2003). Second, combustion of fossil fuels releases gaseous forms of reactive nitrogen, which can be incorporated into aquatic systems through atmospheric deposition (Galloway et al. 2003; Vitousek et al. 1997). Finally, mass production of nitrogen fixing plants, such as soybeans, increases the conversion rate of dinitrogen to reactive nitrogen (Galloway et al. 2003; Vitousek et al. 1997; Donner, Kucharik, and Foley 2004).

1.2. Nitrate in the Mississippi River Basin

Estimates show that the rates of nitrate loading to the Gulf of Mexico by the Mississippi River Basin almost tripled in the period from 1980-1999 as compared to 1955-1970 (Goolsby and Battaglin 2001). The increasing load of nitrate is a major cause of the zone of hypoxia that forms annually in the Gulf of Mexico (Rabalais, Turner, and Wiseman 2002; Goolsby and Battaglin 2001). High nitrate loads cause hypoxia by increasing primary production, which increases decomposition rates and the associated

oxygen consumption (Rabalais, Turner, and Wiseman 2002). The low dissolved oxygen concentrations have many ecological impacts, including alterations to food webs and trophic interactions (Rabalais, Turner, and Wiseman 2002). Inland surface waters are also impacted by increased nitrate levels; effects include acidification of streams and lakes and losses of biological diversity (Vitousek et al. 1997). Additionally, high nitrate levels in drinking water can cause methemoglobinemia ("blue baby syndrome") in infants, in which oxygen transport by blood is inhibited (Lee 1970). Therefore, the U.S. Environmental Protection Agency has set a maximum contaminant level of 10 mg/L nitrate as nitrogen for drinking water ('Ground Water and Drinking Water: National Primary Drinking Water Regulations').

Agricultural settings, especially those in which fertilized corn is grown, are prime locations for high anthropogenic inputs of nitrate. Modeling efforts have demonstrated that a disproportionately high amount of the nitrate exported to the Gulf of Mexico from the Mississippi River Basin is from areas with fertilized crops in the Upper Midwest, including southern Minnesota (Goolsby and Battaglin 2001; Booth and Campbell 2007; Donner, Kucharik, and Foley 2004; David, Drinkwater, and McIsaac 2010; Magner, Payne, and Steffen 2004). More specifically, studies have shown that higher fertilizer inputs are correlated with increased nitrate fluxes (Raymond, David, and Saiers 2012; Booth and Campbell 2007). Furthermore, landscapes with fertilized corn and tile drainage are also correlated with nitrate export (David, Drinkwater, and McIsaac 2010).

Despite high nitrate loading to the Mississippi River and the Gulf of Mexico, not all nitrate that enters the basin's streams is delivered to the Gulf (Alexander, Smith, and Schwarz 2000; Galloway et al. 2003). An assessment of transport of reactive nitrogen in river systems showed that 30% to 70% of nitrogen is removed via denitrification before it reaches coastal systems (Galloway et al. 2003). Biogeochemical processes other than denitrification could also be responsible for nitrate removal (Burgin and Hamilton 2007). This study investigates the removal of nitrate via in-stream processes in the Cottonwood River Watershed, an intensively managed agricultural landscape in southern Minnesota. Because the Cottonwood River Watershed has many of the features that cause high

nitrate export (i.e., fertilized corn cultivation and extensive tile drainage), this study has implications for nitrate loading to the Mississippi River Basin as a whole.

1.3. Study objectives

This study examines water sources, nitrate sources, and nitrate removal processes in the Cottonwood River Watershed. This is accomplished in three steps:

1. A chemical hydrograph separation using an end-member mixing analysis (EMMA) was performed to determine water sources' proportional contributions to the Cottonwood River.
2. A nitrate mass balance calculation was made, in which nitrate concentrations and end-member proportions of streamflow were used to calculate a predicted stream nitrate concentration. The predicted nitrate concentration was then compared to the observed nitrate concentration to assess nitrate removal.
3. An examination of long-term concentration-discharge patterns in the watershed was undertaken to better understand the landscape's nitrate dynamics.

The approach of pairing a chemical hydrograph separation with concentration-discharge analysis is rare, and has only been undertaken by a few other studies (e.g., Liu, Conklin, and Shaw 2017). Combining these two methods is useful because it provides a process-based understanding from the EMMA, but also bolsters the limited temporal scale of the EMMA results with the long-term concentration-discharge analysis.

1.4. Background: chemical hydrograph separation

This study performed a chemical hydrograph separation to determine sources of water and nitrate to the Cottonwood River. Chemical hydrograph separation studies were originally developed to separate precipitation event water from pre-event water (Sklash and Farvolden 1979). Since then, chemical hydrograph separations have been employed in more sophisticated ways, including identification of nitrate sources delivered by atmospheric deposition versus sewage discharge (Divers, Elliott, and Bain 2014), determination of the proportion of streamflow that comes from snow-melt in light of global warming (Maurya et al. 2011; Brooks et al. 2012), study of the depth of soil water sources used by plant communities (Asbjornsen, Mora, and Helmers 2007), and determination of flow pathways to streams (Green et al. 2007).

This study's chemical hydrograph separation examines a variety of possible water sources to the Cottonwood River, determines which are most important, and calculates the proportion of streamflow that each source comprises. The method used in this study for chemical hydrograph separation, end-member mixing analysis (EMMA), involves a multivariate statistical analysis to separate water sources (Christophersen and Hooper 1992). A principal components analysis is employed in order to use information from an unlimited number of chemical tracers, because higher numbers of tracers lend more certainty to the hydrograph separation (Christophersen and Hooper 1992).

EMMA has been used extensively in watershed investigations since its introduction. EMMA has been applied in settings ranging from a karstic region of Italy and Slovenia (Doctor et al. 2006), to a peatland watershed in Alaska (Gracz et al. 2015), to temperate forested watersheds (Ali et al. 2010; James and Roulet 2006). Study questions that have been addressed by EMMA include water source response to wildfire (Jung et al. 2009), nutrient flushing dynamics (van Verseveld, McDonnell, and Lajtha 2008), water source change with catchment scale (James and Roulet 2006), and effect of hydrologic events on water source (Inamdar et al. 2013; Inamdar and Mitchell 2007). Throughout these studies, the methodology introduced by Christophersen and Hooper (1992) and Hooper (2016, 2003) is typically followed, thus providing a consistent basis for comparing results.

1.5. Background: concentration-discharge analysis

Recent research has investigated the relationship between stream discharge and the concentration of a variety of chemical species. Godsey et al. (2009) used long-term concentration-discharge records from a wide variety of watersheds to determine that weathering solutes behave chemostatically with discharge; that is, concentration is approximately constant with discharge on a logarithmic plot. A variety of relationships between the concentration of nitrate and discharge have been demonstrated. In a study that used data from managed catchments in the Mississippi-Atchafalaya River Basin, a positive relationship was found between discharge and nitrate (Basu et al. 2010). This, along with consistent stream water concentrations of nitrate over a time period of

decreased nitrate loading, led authors to conclude that nitrate export was transport limited due to legacy stores of nutrients in the catchment.

Further analysis of nitrate concentration and discharge involved segmenting data records at median discharge and determining the relationship between nitrate concentration and discharge below and above the median (Moatar et al. 2017). This method revealed that below median discharge, logarithmic plots of nitrate versus discharge have a positive slope, but above median discharge, the slope is approximately zero. Investigation into correlations between nitrate concentration and temperature, season, and chlorophyll *a* concentration led authors to conclude that the positive slope at low discharge was due to biogeochemical attenuation of nitrate (Moatar et al. 2017). At higher discharge, such attenuation was thought not to occur because of lower spatial and temporal contact of water with the hyporheic and riparian zones (Moatar et al. 2017).

1.5.1. Weighted Regression on Time, Discharge, and Season model

The relationship between a chemical species' concentration and three predictors—time, stream discharge, and season—was used by Hirsch et al. to model concentration (Hirsch, Moyer, and Archfield 2010). This method, called Weighted Regression on Time, Discharge, and Season (WRTDS), uses daily discharge data and intermittent concentration data to provide daily estimates of concentration during the time period of interest. WRTDS results remove biases in monitoring data caused by oversampling at low or high discharge levels because the model produces concentration estimates for every day. Furthermore, WRTDS results can be used to identify trends through time in concentration-discharge data and relationships.

The WRTDS model has been used by a variety of studies. Many studies have used WRTDS to examine trends in nitrate concentration in agricultural settings, mostly in the Mississippi River Basin (Green et al. 2014; Kelly, Stets, and Crawford 2015; Sprague, Hirsch, and Aulenbach 2011; Kreiling and Houser 2016). The WRTDS model has also been used to examine concentrations of phosphorus, suspended sediment, and chloride (Corsi et al. 2015; Kreiling and Houser 2016). When compared to measured loads of nitrate in the Mississippi River, the WRTDS model performed well over the course of a two-year study, with underestimates of only approximately 3.5% (Pellerin et al. 2014).

However, results from monthly time-steps revealed less accurate estimates by the WRTDS model (Pellerin et al. 2014).

This study utilized the WRTDS model in order to augment nitrate concentration datasets so that the concentration-discharge relationship of nitrate in the Cottonwood River Watershed could be more effectively analyzed. Trends in the concentration-discharge relationship over time were also examined using WRTDS methods.

2. Study Area

2.1. Geology

The Cottonwood River, located in southern Minnesota, is a tributary to the Minnesota River (Figure 1). Geologically, the area is underlain by Archean metamorphic bedrock, which is cut by intrusions of igneous rocks (Boerboom 2016; Jirsa 2016). Above the metamorphic rock is a thin (approximately 45 m) layer of Cretaceous interbedded mudstones, shales, and sandstones, which is often used as a drinking water aquifer in the region (Jirsa 2016). This unit becomes thinner and less continuous to the east of the watershed. In the eastern area of the watershed near New Ulm, the Cambrian Mt. Simon Sandstone is also present (Boerboom 2016).

The watershed is overlain by approximately 15 to 90 m of glacial sediment, deposited during multiple glaciations (Knaeble 2016; Gowan 2016a). Most surficial glacial sediment in the region was deposited during the most recent glaciation, the Late Wisconsinan, which ended approximately 10,000 years ago (Hobbs 2016). During that period, the area was occupied by the Des Moines Lobe of the Laurentide ice sheet, which repeatedly advanced and retreated, depositing a series of glacial sediments during the process (Hobbs 2016; Patterson 1997). The Cottonwood River formed during one of these retreats; as ice retreated to the northwest, meltwater created flow along the approximate path of the present-day river (Hobbs 2016). Deeper glacial sediments are derived from previous glaciations (Knaeble 2016; Gowan 2016a).

Cross sections of the Quaternary material in the region show that the majority of Quaternary sediment deposited by the Des Moines Lobe and by pre-Wisconsinan glaciations in the region is till (Knaeble 2016; Gowan 2016a). Outwash sands and gravels were also deposited by sub- and pro-glacial streams; however, these deposits are less

dominant because more area was covered by till-depositing ice than by streams (Gowan 2016a). The Cottonwood River is underlain by these sands and tills. Cross sections indicate that slightly upstream of Lamberton, approximately 15 m of glacially-deposited sands underlie the river valley, but the depth of these sands appears to decrease significantly downstream to only 0 to 3 m near Leavenworth (Gowan 2016a; Knaeble 2016). Beneath the sands, up to 30 m of glacial till is present (Gowan 2016a; Knaeble 2016).

2.2. Topography

A notable geomorphologic feature in the region is the Coteau des Prairies (henceforth referred to as the Coteau), which is a plateau of higher elevation that extends from South Dakota into southwest Minnesota, trends northwest-southeast, and becomes less prominent to the southeast. The Coteau is an erosional feature that was carved out by the Des Moines Lobe to the northeast and by the approximately coeval James Lobe to the southwest during advance of both lobes (Patterson 1997; Hobbs 2016). It is thought that the two lobes separated around the Coteau due to a topographically higher area of metamorphic bedrock (Hobbs 2016). The Coteau plays an important role in the hydrology of the Cottonwood River Watershed. Streams that drain the Coteau make up the majority of the watershed's tributaries ("Minnesota River - Cottonwood River Watershed"). Furthermore, the Coteau creates a steep gradient in water table elevation, causing a northeastern direction of groundwater movement in the area (Bradt 1997). The average gradient of the river is 1.4 m/km; however, the steepest reaches occur upstream near the Coteau, where the gradient reaches approximately 7.6 m/km. ("Watershed Context Report: Cottonwood River" 2017).

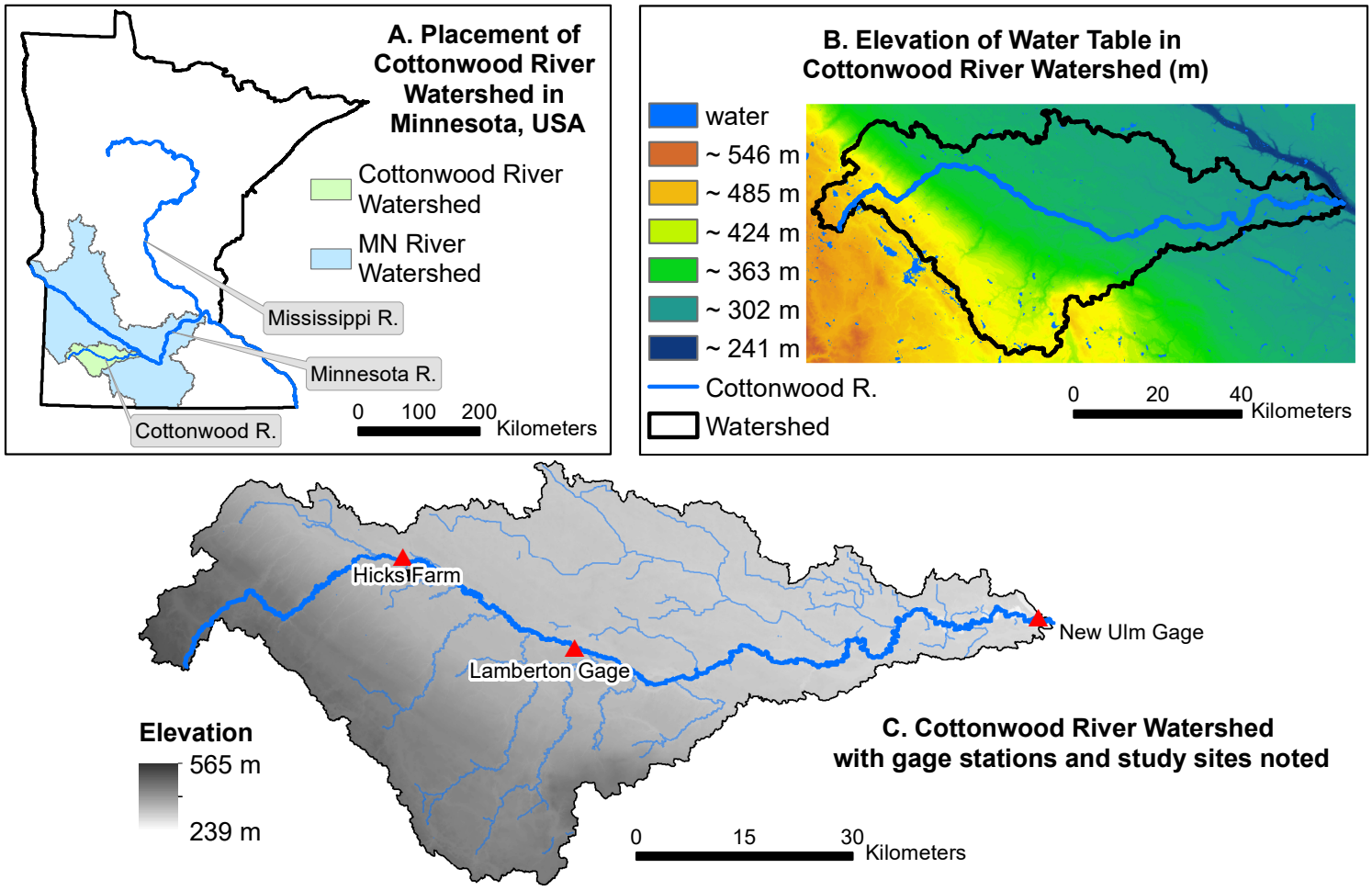

Figure 1. Cottonwood River Watershed study area. ("County Boundaries, Minnesota" 2013; "MNDNR Hydrography" 2018; "MNDNR Watershed Suite" 2018; "Water-Table Elevation and Depth to Water Table, Minnesota Hydrogeology Atlas series HG-03" 2016; "Minnesota Digital Elevation Model - 30 Meter Resolution" 2018)

2.3. Land use

Land use in the Cottonwood River Watershed is predominantly agricultural. According to 2011 National Land Cover Database aerial data, cultivated cropland occupies 84.9% of the watershed ("Watershed Context Report: Cottonwood River" 2017). The next-largest category is 4.9% developed open space ("Watershed Context Report: Cottonwood River" 2017). The watershed's population density is low, at 8.58 people per square km ("Watershed Context Report: Cottonwood River" 2017). The biggest population center is the city of New Ulm, at the outlet of the watershed ("Watershed Context Report: Cottonwood River" 2017). The percentage of impervious land in the watershed is also low, at 0.71% ("Watershed Context Report: Cottonwood River" 2017).

Crop cover data show that, in 2016, 40.3% of the watershed was planted in corn and 37.9% of the watershed was planted in soybeans ("Watershed Context Report: Cottonwood River" 2017). To accommodate agricultural land use, significant drainage alterations have been made, including straightening and ditching of watercourses ("Watershed Context Report: Cottonwood River" 2017). Within the watershed, 38.8% of watercourses are natural, while 40.8% have been physically altered ("Watershed Context Report: Cottonwood River" 2017). Draining of wetlands using agricultural tile drainage is also prevalent in the region ("Watershed Context Report: Cottonwood River" 2017). Loss of wetlands can be evaluated through the extent of hydric soils, which form under conditions of extended saturation during the growing season. Therefore, the present distribution of hydric soils indicates areas where wetlands once existed prior to artificial drainage ("Watershed Context Report: Cottonwood River" 2017). The Cottonwood River Watershed is composed of 47.4% hydric soils but only contains 3.4% wetlands; this large difference can be interpreted to represent substantial wetland loss due to artificial drainage ("Watershed Context Report: Cottonwood River" 2017). Tile drainage and ditching have significant geomorphic and water quality consequences (Lenhart et al. 2012; Schottler et al. 2014).

2.4. Climate

Annual precipitation in the watershed ranges from 64 cm on the western side of the watershed to 69-74 cm on the eastern side ("Rapid Watershed Assessment Resource Profile: Cottonwood (MN) HUC: 7020008"). At Lamberton, average precipitation (calculated from 1961 to 2017) is 68 cm, and in 2017 annual precipitation was 76 cm (University of Minnesota: Southwest Research and Outreach Station - Lamberton 2018). Soil moisture monitoring at Lamberton shows that typically, soil moisture peaks in mid-June and is lowest at the beginning of September; however, in 2017 soil moisture peaked in the beginning of May and was lowest in mid-July (University of Minnesota: Southwest Research and Outreach Station - Lamberton 2018). Temperatures at Lamberton range from January average minimum and maximum of -15.5°C and -5.0°C, respectively, to July average minimum and maximum of 16.4°C and 28.6°F, respectively (calculated from years 2008 to 2017) ("Climate Data for Lamberton Southwest Research and Outreach Center" 2018).

2.5. Sample collection sites

Samples were collected from a variety of water sources at multiple sites in the Cottonwood River Watershed (Figure 2). At the Hicks Farm site, tile drainage and riparian water were collected. Three river-miles upstream of the Lamberton gage, riparian water from two areas, spring water, and stream water were collected. Long-term concentration and discharge data recorded at the Lamberton gage and the New Ulm gage were also used (Figure 1). Watershed area at Lamberton is 1150 km^2 (MNDNR 2014), and at New Ulm is 3326 km^2 ("Minnesota River - Cottonwood River Watershed").

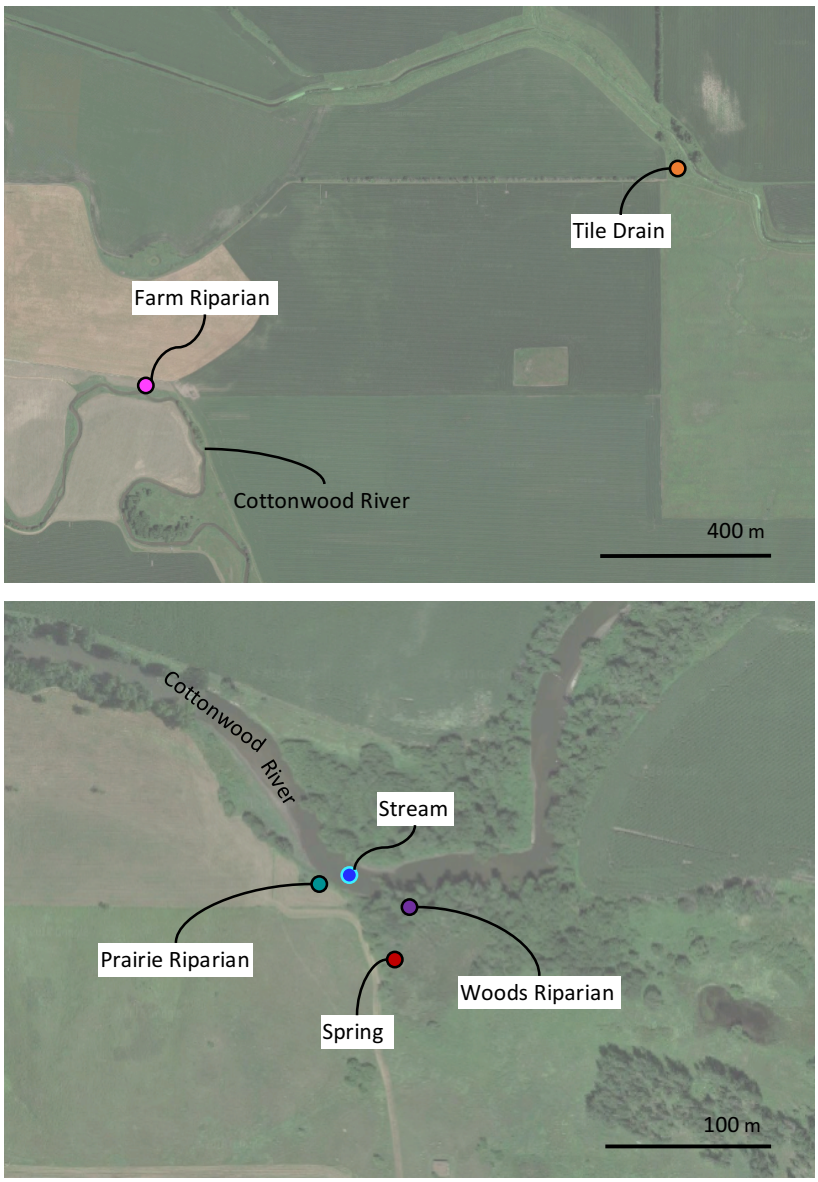

Figure 2. Hicks Farm site (top) and Lamberton sampling site (bottom). The Lamberton sampling site is approximately 3 river miles upstream from the Lamberton gage. (Map data: Google, 2018).

3. Methods

3.1. Field and laboratory methods

3.1.1. Sample collection

Water samples were collected from stream, tile drainage, spring water, and shallow riparian groundwater for analysis of nitrate plus nitrite as N (NO_{2+3}^--N), cation (Ca^{2+}, K^+, Mg^{2+}, Na^+, Si^{4+}), and anion (NO_3^-, NO_2^-, Cl^-, SO_4^{2-}) concentrations (locations shown in Figure 2). For stream water collection, a swing-sampler was used to facilitate collection of water that was actively moving in the stream channel. Tile drainage was pumped from an underground tile main using a peristaltic pump. The pump tubing was pre-rinsed with sample water to clear it of any contamination prior to sample collection. Spring water collection was facilitated by a polyvinyl chloride (PVC) pipe (5.1 cm diameter and 1.5 m long) that had been stuck into the spring about a month before sample collection commenced. Spring water flowed continuously out of the pipe, enabling sample collection.

Shallow riparian groundwater was sampled from PVC pipe wells that had been augured into the ground, back-filled with sand, and sealed at the top with bentonite during the previous fall. PVC pipes were either 1.5 or 3.0 m long (depending on the depth to the water table), and were 5.1 cm in diameter. The bottom 1.5 m of each PVC pipe well was open to the surrounding groundwater via thin slotted holes. PVC pipes were situated in the riparian zone of the stream, within approximately 15 m of the stream. Wells were sampled using two methods: (1) without purging the standing water in the well, or (2) purging the standing water until wells were dry or until over one full volume of water had been evacuated from the well. Results from the two methods were compared in order to determine which data to use; if the non-purged chemical concentrations were sufficiently similar to the purged concentrations then both methods were used, otherwise only data from the purged method was used.

All samples were stored in 30-mL high density polyethylene (HDPE) bottles. The sample bottles were either brand new (never previously used) or were cleaned between samples using an acid wash method adapted from the U.S. Geological Survey (USGS) ("Cleaning of Equipment for Water Sampling" 2004). The acid washing procedure

involved first washing bottles with 0.1% to 2% volume/volume non-phosphate laboratory grade detergent, and then soaking bottles in 5% volume/volume hydrochloric acid (HCl) solution for 30 minutes. Following the soak in HCl, bottles were rinsed in deionized water until the pH of the rinse water was neutral. Bottles were allowed to air dry completely, and were stored in a clean area away from contamination.

Water samples were collected in a Nalgene brand HDPE bottle that had the top cut off to allow for easy access and cleaning. The bottle was thoroughly cleaned with deionized water and completely dried with a laboratory-grade tissue between each sample. Upon sample collection, water temperature, conductivity, pH, and dissolved oxygen (as a percent) were measured using a YSI 6820 V2 multi-parameter water quality sonde. Sonde sensors were cleaned with deionized water and dried with a laboratory grade-tissue between each sample. Immediately following sonde measurements, water samples were filtered into sample bottles using a nylon 0.45-micron filter and a 20-mL plastic syringe. A new or clean syringe was used for each sample. When syringes were reused, they were washed using the same acid wash protocol as sample bottles. Minimal headspace was left in sample bottles to prevent interaction with air in the bottle.

3.1.2. Sample preservation

Sample preservation was achieved through chilling at approximately 4°C and acidification of cation samples. In the field, samples were stored in a cooler with ice for preservation. Upon return to the lab (within ten hours), samples were stored in a dark refrigerator at approximately 4°C. Also upon return to the lab, cation samples were acidified using two drops of 6 normality HCl solution for each 30 mL sample, in a method adapted from the Standard Methods for Water and Wastewater (American Public Health Association 1960). This procedure mimicked the procedure used for samples collected for the Minnesota Department of Natural Resources (MN DNR) groundwater chemistry database (Alexander 2018). Because samples from this database were also used in the end-member mixing analysis, it was important to ensure consistency between sample preservation procedures so that data from both sources were comparable.

3.1.3. Sample analysis

Samples collected for nitrate concentration were analyzed using a Hach Nitratax *plus sc* probe, which measured nitrate plus nitrite as nitrogen (NO_{2+3}^--N) in mg/L. The probe uses UV absorption to measure nitrate plus nitrite concentration in water, taking advantage of the fact that dissolved nitrate plus nitrite absorbs UV light at wavelengths below 250 nm (Hach 2014). The probe measures concentrations from 0.1 mg/L to 50 mg/L NO_{2+3}^--N, which was sufficient for all samples presented in this study. The probe has a mechanism to compensate for turbidity, though this was not necessary because all samples were filtered through a 0.45-micron filter before analysis. The probe's measuring error is 3% of the measured value ± 0.5 mg/L (Hach 2014).

Samples collected for cation and anion concentration were analyzed by Elizabeth Lundstrom, a technician at the Geochemical Laboratory at the University of Minnesota's Department of Earth Sciences. Analyses were always completed within 28 days of sample collection. Cation analysis was performed using inductively coupled plasma optical emission spectrometry (ICP-OES) on a Thermo Scientific iCAP 6000 Series spectrometer. For each sample, three ICP-OES runs were performed. Each run, in turn, consisted of five individual measurements. Average concentrations for the three runs were used for each sample. Anion analysis was performed using a Thermo Scientific Dionex ICS-5000+ ion chromatography system. Each sample was run twice and averages were used.

3.1.4. Probe calibration

Temperature, conductivity, pH, and dissolved oxygen were measured for each sample using a YSI 6820 V2 multi-parameter water quality sonde. The sensors for these parameters were calibrated according to the YSI probe manual directions (YSI 2012). Conductivity was calibrated weekly using a one-point calibration with 1.413 mS/cm calibration fluid. Every day that the sonde was used, pH was calibrated using a two-point method with pH 7 and pH 10 calibration fluids. Dissolved oxygen was calibrated each day that the sonde was used by equilibrating the sensor to barometric pressure. Between all calibrations, the sonde sensors were rinsed with deionized water and thoroughly dried with a laboratory-grade tissue. Although sonde results were not used directly in analysis,

they were helpful in confirming that physiochemical parameters of the water samples were within expected ranges.

The Hach Nitratax *plus sc* probe for nitrate measurement was also calibrated regularly to ensure accurate readings, following directions in the probe's manual (Hach 2014). Calibration was achieved using a two-point method. Calibration of 0 mg/L NO_{2+3}^--N was performed using deionized water. A 50 mg/L NO_{2+3}^--N standard by Aqua Solutions, Inc., was used for the second calibration point. Every time the Nitratax probe was used, both calibration fluids were measured on the Nitratax probe to check the calibration for each. If either measurement was outside the error range for the probe of 3% of the measured value ± 0.5 mg/L, the probe was recalibrated such that measurement of calibration fluids were within the error range.

3.1.5. Quality assurance and control measures

Nitrate plus nitrite samples were typically collected in triplicate (i.e., three samples were collected for each water source) and all three were analyzed for NO_{2+3}^--N concentration using the Nitratax probe. The average of the three sample concentrations was used to represent nitrate concentration in the sample. Triplicate samples were not taken for the field blank and for four other samples. To ensure that the measurement of NO_{2+3}^--N from the Nitratax probe was accurate, ion chromatography results from six duplicate samples from the May 30, 2017 sampling campaign were compared to the Nitratax probe results. Ion chromatography was performed on June 2, 2017 (two days after Nitratax probe analysis was performed). Results of this comparison can be found in Table A-1 of the Appendix. All differences between the two analysis methods were within the error range for the Nitratax probe. Based on this comparison, it was determined that using the Nitratax probe for subsequent nitrate samples was appropriate.

A field blank sample consisting of deionized water was taken into the field on one sample date to assess the extent of contamination during the field procedure. The field blank sample was subjected to all the same processes as normal samples, including pumping by the peristaltic pump, temporary storage in the Nalgene bottle, physical parameter testing using the YSI sonde, filtration using the 0.45-micron filter and syringe system, and storage in the 30-mL sample bottles in the same cooler and refrigerator as the

other samples. The results of the field blank tests are presented in Table A-2 of the Appendix. These concentrations, though low, may be used as indications of possible levels of contamination in the samples.

3.2. End-member mixing analysis

3.2.1. Statistical methods

An end-member mixing analysis, or EMMA, was employed to separate stream flow into end-members and find the proportion of stream flow that each end-member composed (Christophersen and Hooper 1992; Hooper 2003). In traditional hydrograph separation, for *n* sources, *n-1* tracers should be used to exactly constrain their contributions (Klaus and McDonnell 2013). The tracer concentrations are used to solve for end-member proportional contributions to streamflow in the following system of equations (developed here for a system with two tracers, C1 and C2, and three water sources, Q_1, Q_2, and Q_3) (Klaus and McDonnell 2013):

$$Q_t = Q_1 + Q_2 + Q_3 \quad (1)$$

$$C1_tQ_t = C1_1Q_1 + C1_2Q_2 + C1_3Q_3 \quad (2)$$

$$C2_tQ_t = C2_1Q_1 + C2_2Q_2 + C2_3Q_3 \quad (3)$$

Mathematically, this limits the number of tracers that can be used without over-constraining the problem. There are usually more tracers available for measurement than can be used mathematically, and it is advantageous to incorporate more than the minimum number of tracers into the mixing model because this will enable the model to represent more sources of variation in water chemistry. EMMA removes the limitation on number of tracers used by applying principal components analysis (PCA) (Christophersen and Hooper 1992). PCA reduces the dimensionality of the tracer data by extracting the most important information from the tracers. The lower dimensional space defined by the principal components is termed U-space. The principal components are used to solve for end-member proportional contributions to streamflow in a system of equations equivalent to equations 1 through 3 (above), but in which principal component values have been substituted for tracer concentrations (Burns et al. 2001).

EMMA was carried out following the steps outlined by Hooper (Hooper 2003, 2016). First, a matrix of the stream sample data was created, where rows were samples taken and columns were tracers. Means and standard deviations for each tracer were calculated, and were used to create a correlation matrix by subtracting the mean and dividing by the standard deviation for each element in the matrix. This step prevents any tracer from having a disproportionate effect on the PCA due to differences in scaling or variation (Hooper 2003). PCA was performed on the correlation matrix of stream data in the statistical software R version 3.4.1 ("R: A Language and Environment for Statistical Computing" 2017) using the *prcomp()* command, which uses singular value decomposition to extract the eigenvectors and associated eigenvalues from the matrix. The eigenvalues give information on how much of the data's variance each eigenvector describes. Therefore, the number of eigenvectors chosen to describe the data as principal components was guided by the proportion of variance that each eigenvector describes. This reasoning, called the Rule of One, indicates that each eigenvector designated as a principal component should explain at least as much as $(\frac{1}{n} * 100)\%$ of the variation in the data, where *n* is the number of eigenvectors total (Hooper 2003). Because the principal components are used in equations 1 through 3 to solve for the proportions of each end-member in the stream water, if *n* principal components are selected, *n+1* sources of water to the stream are considered.

The PCA described above found a U-space that was defined by the stream chemistry data. The potential end-members were then projected into this U-space. Specifically, median tracer concentrations for each end-member were standardized using the stream data means and standard deviations, and projected into U-space through matrix multiplication of the eigenvector loadings by the transpose of the standardized end-member matrix (Burns et al. 2001; Hooper 2016). Examination of a plot of all stream and end-member data in U-space allowed for the selection of end-members that bounded the stream data (Burns et al. 2001; Christophersen and Hooper 1992). Selection of end-members was further determined by comparing the distance from the U-space plane to each end-member before projection into U-space; end-members with a smaller distance were favored (Christophersen and Hooper 1992).

After end-members were chosen, the proportion of streamflow that each end-member composed was calculated using equations 1 through 3. All stream data was bounded by the end-members, so no projection of stream data points onto the borders of the mixing triangle was necessary. Projection of stream data points onto the nearest edge of the mixing triangle would have been performed if stream data had plotted outside the triangle, in order to prevent any end-member from having a negative contribution to streamflow (Hooper 2016).

An error analysis was performed on the end-member data in principal components space as follows: all end-member data points were plotted in principal components space, and the interquartile range (or the overall range for the tile drain end-member, where only two samples were taken) for principal component one and two was calculated. The interquartile range for end-members is represented by the error bars in the mixing space plot. This approach followed methods described by Bernal, Butturini, and Sabater (2006) and Jung et al. (2009). Interquartile ranges were then propagated through the analysis of fractional end-member contributions to streamflow by considering the four most extreme possible end-member points defined by the error bars. Every combination of these four points for each end-member was run through the EMMA calculations, for a total of 64 end-member contribution scenarios. These scenarios were used to calculate interquartile ranges for nitrate reduction values, which were also plotted as error bars. The concept of testing many possible end-member contribution scenarios to quantify uncertainty in EMMA was also used by Bernal, Butturini, and Sabater (2006). For stream samples, analytical standard deviations were plotted as error bars using the equation for quantifying uncertainty in principal component space given by Hooper et al. (2001). Error bars that represent one standard deviation in principal components one and two were plotted, but were not propagated through subsequent analysis because they were typically very small (often within the bounds of the point on the graph).

Many EMMA studies perform a residual analysis in which data points that have been projected into U-space are compared with original data in concentration units (Hooper 2003). The residuals are calculated as the difference between the projected and the original data. Random structure in a residuals plot indicates that the number of

eigenvectors chosen to represent the data was sufficient (Hooper 2003). However, this approach was not used here, because six stream data points are not adequate to confidently glean information from the structure of a residuals plot.

Tracers were selected based on an assessment of bivariate plots, in which each combination of tracers was plotted against each other. Approximately linear relationships between tracers implies, though does not prove, conservative behavior by tracers (Hooper 2003). Tracer selection was also limited by the chemical species that were included in the datasets for groundwater and precipitation chemistry in the area.

3.2.2. Data used

The data used for the end-member mixing analysis is described in Table 1. This study's sampling data was used for cation, anion, and nitrate plus nitrite concentrations in the stream, tile drainage, shallow riparian groundwater, and spring water in the Cottonwood River Watershed. For water chemistry of the Quaternary aquifer in the region, the Minnesota Department of Natural Resources (MN DNR) database of groundwater chemistry was used ("MN Department of Natural Resources: Water Chemistry Data" 2017). Three wells with complete cation and anion analyses were selected to represent Quaternary groundwater based on the positions in the Quaternary aquifer in which they were screened. Nitrate concentrations from Quaternary groundwater were determined from two of the wells in the MN DNR's database, along with nine wells from the Minnesota Well Index, which is provided by the Minnesota Department of Health and the Minnesota Geological Survey ("Minnesota Well Index"). These wells were also in Quaternary aquifers in the region. All Quaternary aquifer chemistry is from a region that contributes hydrogeologically to the Cottonwood River at Lamberton or upstream of Lamberton, according to the northeastern movement of groundwater in the region (Bradt 1997). Of the 11 wells with nitrate concentrations used, nine of the results were below detection level. Quantification of the median nitrate concentration was difficult due to both the high proportion of censored data and the fact that three different detection levels in the dataset existed. Therefore, half the detection level was substituted for all censored values and the median of the new dataset was used.

Precipitation chemistry was attained through the National Atmospheric Deposition Program (NADP)'s site at the University of Minnesota's Southwest Research and Outreach Station at Lamberton, MN ("National Atmospheric Deposition Program: National Trends Network, Lamberton, MN" 2017). Weekly data was downloaded for the time period from January 1996 to December 2016 from the NADP website, and medians for the weeks in May through September were calculated for the chemical constituents of interest. Silica was not available via NADP data, so an average concentration of silica in precipitation in Iowa was used (Anderson and Downing 2006).

Tile drainage nitrate concentrations were supplemented with data from a previous study. Due to access limitations, the tile main on a private farm in the Cottonwood River Watershed was only sampled twice for cation and anion concentrations and three times for nitrate concentrations as part of this study. Nitrate concentrations from the same tile main collected in 2006, 2008, and 2009 were therefore used for May and June tile drainage nitrate values (Ranaivoson 2018). Cation and anion concentration results from this study's two sampling events were assumed to be representative of the entire study period, because they were very consistent despite contrasting antecedent precipitation conditions. Specifically, precipitation records from the city of Tracy (11.7 km southwest of the tile main) show that there were 0.08 cm of rain in the four days prior to the first sampling date and 9.9 cm of rain in the four days prior to the second sampling date ("Climate Data for Tracy" 2018).

Table 1. Data used for end-member mixing analysis.

Data Used: End-Member Mixing Analysis					
Water Source	**Site Description**	**Cation and Anion Concentrations**		**Nitrate plus Nitrite Concentrations**	
		Data source	**Dates sampled**	**Data source**	**Dates sampled**
Stream	University of MN Southwest Research and Outreach Station at Lamberton, MN	This study's sampling data	6 sampling dates (5/30/17, 6/13/17, 6/27/17, 7/11/17, 7/24/17, 9/17/17)	This study's sampling data	6 sampling dates (5/30/17, 6/13/17, 6/27/17, 7/11/17, 7/24/17, 9/17/17)
Tile drainage	Tile main at privately owned farm at 44°20'37.67" N, 95°32'55.61"W	This study's sampling data	2 sampling dates (7/11/17, 7/24/17)	This study's sampling data; additional data from 2006 - 2009	This study's data: 3 sampling dates (7/11/17, 7/24/17, 9/17/17) Additional data from May-June 2006 - 2009
Shallow riparian groundwater	Riparian sites (within apprx. 50 ft of river) at privately owned farm at 44°20'37.67"N, 95°32'55.61"W and at the University of MN Southwest Research and Outreach Station at Lamberton, MN	This study's sampling data	Woods Riparian: 6 sampling dates (5/30/17, 6/13/17, 6/27/17, 7/11/17, 7/24/17, 9/17/17); Farm Riparian: 2 sampling dates (7/24/17 and 9/17/17); Prairie Riparian: 1 sampling date (9/17/17)	not used	not used
Spring water	Naturally occuring spring at the University of MN Southwest Research and Outreach Station at Lamberton, MN	This study's sampling data	5 sampling dates (5/30/17, 6/27/17, 7/11/17, 7/24/17, 9/17/17)	This study's sampling data	6 sampling dates: (5/30/17, 6/13/17, 6/27/17, 7/11/17, 7/24/17, 9/17/17)
Quaternary Groundwater	Wells in Quaternary buried artesian aquifer (47 to 390 ft deep) in region that contributes hydrogeologically to the Cottonwood River at or upstream of Lamberton, MN. Aquifer identification by MN Geological Survey.	MN Dept. of Natural Resources well chemistry data (wells 212954, 196772, and 196761)	May 1994 to May 1995	County Well Index (9 wells) and MNDNR well chemistry data (2 wells)	County Well Index: April 2006 to Sept. 2013 MNDNR wells: Oct. 1994 and May 1995
Precipitation	Data from the National Atmospheric Deposition Program (NADP) site at the University of MN Southwest Research and Outreach Station at Lamberton, MN was used for Ca^{2+}, Mg^{2+}, Na^{+} and NO_3^{-} concentrations. Medians from May through Sept. for 1996 through 2016 were used. Si^{4+} concentrations were from a study in Iowa that recorded atmospheric depostion (Anderson et al. 2006).				

3.3. Alternative hydrograph separation methods

Hydrograph separation was performed using a variety of methods that utilize streamflow records to distinguish various components of the hydrograph. Each of these hydrograph separation techniques was applied to daily streamflow data from the 2016 and 2017 calendar years in the Cottonwood River at the MN DNR Lamberton stream gage.

3.3.1. PART

The PART computer program, developed by the U.S. Geological Survey, was applied to Lamberton streamflow data. PART uses an algorithm that determines baseflow based on antecedent streamflow recession (Rutledge 1998). Daily baseflow estimates that satisfied PART's second antecedent recession requirement, which yields an intermediate estimate of baseflow of the three possible antecedent recession requirements, were used (Rutledge 1998).

3.3.2. Lyne and Hollick digital filter

Baseflow separation via the Lyne and Hollick digital filter was also performed on Lamberton streamflow data (Lyne and Hollick 1979). This method uses an equation to separate baseflow from overall stream discharge under the assumption that baseflow displays low frequency signals and quickflow displays high frequency signals (Nathan and McMahon 1990). The method is not based on physical processes that control baseflow, but has been used extensively regardless (Ladson et al. 2013). The 'hydrostats' package (Bond 2016) in the statistical software R was used for this analysis ("R: A Language and Environment for Statistical Computing" 2017). Parameters used for this analysis were alpha of 0.925, which has been widely used in the Lyne and Hollick digital filter algorithm (Nathan and McMahon 1990) and reflected number of dates to condition the filter of 30, which is the default parameter provided by the 'hydrostats' package and has also been recommended for widespread use (Bond 2016; Ladson et al. 2013).

3.3.3. Eckhardt digital filter

The Eckhardt digital filter, which is an adaptation of the Lyne and Hollick digital filter, was also applied to Lamberton streamflow data (Eckhardt 2005, 2012). The Eckhardt filter is thought to be an improvement of the Lyne and Hollick filter because it

allows baseflow and streamflow to decrease over time when quickflow is discontinued, which the Lyne and Hollick filter does not accomplish (Eckhardt 2005). The Eckhardt filter was implemented using the 'Flowscreen' package (Dierauer and Whitfield 2017) in the statistical software R ("R: A Language and Environment for Statistical Computing" 2017). Parameters used for the Eckhardt digital filter were a recession constant value of 0.970 and a maximum baseflow index (BFI_{max}) of 0.80, based on values recommended for "perennial porous aquifer streams" (Eckhardt 2012).

3.3.4. Recession curve method

Finally, a graphical technique to separate various water sources based on the recession limb of a hydrograph peak was applied to five recession periods from 2016 to 2017. This technique involves identifying recessions of various contributing sources to the stream in a semilogarithmic plot (Linsley Jr., Kohler, and Paulhus 1958). This method was originally suggested by B. S. Barnes (1940), and will be referred to as the Barnes method henceforth. The slopes of the recession curves were compared in order to better understand the variety of water sources that may contribute to the Cottonwood River.

3.4. Concentration-discharge analysis

3.4.1. Data used

Analysis of long-term concentration-discharge data throughout the watershed was undertaken to better understand the watershed's nitrate dynamics. Simultaneous (same day) data on nitrate concentration and daily discharge in two locations in the Cottonwood River Watershed, Lamberton and New Ulm, were used (Figure 1). At Lamberton, 211 concentration-discharge data points spanning from 2000 to 2012 were available; at New Ulm, 588 concentration-discharge data points from 1997 and 2000 to 2017 were available. See Table 2 for more details.

Discharge data at Lamberton are provided by the MN DNR, and at New Ulm by the USGS. At Lamberton, stage is measured using a Design Analysis Associates pressure sensor/data logger and Gas Purge System in a housing (MNDNR 2014). At New Ulm, primary stage readings are taken by a Design Analysis Associates H-3613i radar water-level sensor. Additional stage data are also available via a Sutron CF pressure transducer/bubble system in a housing. Prior to June 2, 2016, stage at New Ulm was read

via a stilling well. Discharge data are not affected by the change in equipment because of the stage measurements are accurate to 0.30 cm (Kessler 2018).

Data on nitrate concentration at Lamberton and New Ulm are available from the Minnesota Pollution Control Agency (MPCA) on their Environmental Data Access webpage. Samples were processed at labs at the Minnesota Department of Health, Minnesota Valley Testing Laboratory, or Minnesota State University at Mankato. The analytical method used was EPA Method 353.2: Determination of Nitrate-Nitrite Nitrogen by Automated Colorimetry. This method measures inorganic nitrogen (nitrate plus nitrite) as N. The reporting limit for this laboratory method is 0.2 mg/L NO_{2+3}^{-}-N, and data below this concentration was reported as <0.2 mg/L NO_{2+3}^{-}-N. In the Lamberton data set, 14.7% of the concentration data were censored, and in the New Ulm data set, 5.3% of the concentration data were censored.

Table 2. Data used for concentration-discharge analysis and WRTDS model.

Data Used: Concentration-Discharge (CQ) Analysis						
Site	**Latitude/ Longitude**	**Drainage Area (km^2)**	**Date Range**	**Number of CQ Data Pairs**	**Data Provider**	**WRTDS Model**
Lamberton	44° 14’ 19” N 95° 14’ 43”W	1150.1	2000 to 2012	211	MN DNR	Modelled from 2000 to 2012. Winter flow data was not available during from 2000 to 2012; however, winter flows were estimated using a linear regression relationship between New Ulm winter flows and Lamberton winter flows from 2013 to 2017 (R^2 = 0.76 for Nov.-Dec.; R^2 = 0.73 for Jan.-Feb.; R^2 = 0.87 for Mar. - April).
New Ulm	44° 17' 21" N 94° 26' 21" W	3325.5	1997 2000 to 2017	588	USGS and MN DNR	Modelled for 1997 to 2017; all necessary data was available.

3.4.2. Weighted Regression on Time, Discharge and Season analysis

To examine patterns in nitrate concentration in the Cottonwood River Watershed, the Weighted Regression on Time, Discharge and Season (WRTDS) model was used (Hirsch, Moyer, and Archfield 2010). The WRTDS model is part of the USGS's "Exploration and Graphics for RivEr Trends" package for use in R statistical software ("R: A Language and Environment for Statistical Computing" 2017)

The WRTDS model uses a statistical method to estimate the concentration of an analyte of interest, in this case nitrate, for every day during the record of concentration and discharge (Hirsch, Moyer, and Archfield 2010). This is achieved through a regression equation that expresses the concentration as a function of four components: discharge, time trend, season, and random variation. The regression equation is in the following form:

$$\ln(c) = \beta_0 + \beta_1 t + \beta_2 \ln(Q) + \beta_3 \sin(2\pi t) + \beta_4 \cos(2\pi t) + \varepsilon$$

where the β values are fitted coefficients, c represents concentration of the analyte of interest, Q represents daily discharge measurements, t represents time (years), and ε represents the variation that is not explained by the model (Hirsch, Moyer, and Archfield 2010). The model uses existing concentration and discharge data to estimate daily nitrate concentrations based on a weighted moving window, such that observations that are closer to the date to be estimated in terms of discharge level, year, and season have more weight in the estimate than those that are further away. The weighted moving window is implemented using Tukey's tri-cube weighting function.

For each of the components in the regression equation, a half-window width must be set to determine the breadth of data that will contribute to the estimate at any given date. The half-window widths recommended by the model's manual were used (Hirsch and De Cicco 2015). For discharge, a half-window width of $\ln(Q) = 2$ was used (where Q is measured in m^3/s). For time, a half-window width of 7 years was used. For season, a half-window width of 0.5 years was used; this means that all data points influence the regression, but due to the weighting function, points that are around half a year away from the estimate have a very small impact on the regression.

Datasets that span 20 years or more and have at least 200 concentration-discharge data pairs are best suited for the WRTDS model. However, it can also be applied to datasets that only span 10 years and have as few as 60 concentration-discharge data pairs (Hirsch and De Cicco 2015). Nonetheless, daily discharge values are required for the entire period of analysis (Hirsch and De Cicco 2015). The concentration-discharge data available at New Ulm was ideal for the WRTDS model (see Table 2); however, the Lamberton dataset needed adjustment because there were multi-month gaps in discharge data at Lamberton during winter (typically late November through early April). In order to model Lamberton using WRTDS without winter discharge data, two measures were taken: missing winter discharge was estimated at Lamberton using a linear regression relationship between Lamberton and New Ulm winter flows, and a sensitivity analysis to determine the effect of incorrect winter flows on WRTDS results was performed.

To develop a linear regression relationship between New Ulm and Lamberton flows, data from November 20 through April 10 for years during which some or all of winter discharge data was recorded (2000, 2007, 2010, and 2012 through 2017) was used. The winter season was segmented into three time periods: November 20 through December, January and February, and March through April 10. For each period, average daily discharge at Lamberton was plotted against average daily discharge at New Ulm and a linear best fit line was found. The regression equations and associated R^2 values are listed in Table A-3 of the Appendix. These equations were then used to estimate daily discharge values at Lamberton during the months when discharge data were not available.

A sensitivity analysis was also performed to determine the impact of incorrect winter discharge data on WRTDS concentration estimates. Theoretically, incorrect discharge data for dates on which concentration data is not available should not affect the regression equation, because only dates for which there is both concentration and discharge data are used to derive the regression coefficients. WRTDS estimates of concentration on dates with incorrect discharge data will be incorrect, because the wrong discharge value will be input into the regression equation. However, omitting estimates

from these dates from any subsequent analysis will prevent this issue from affecting conclusions.

To confirm that incorrect discharge data posed little concern to model results for dates on which correct discharge data was available, a sensitivity analysis on the New Ulm site was performed. The New Ulm site was examined because complete discharge data throughout the entire year was available there; thus, model results for true discharge values and incorrect discharge values could be compared. Two WRTDS models were run for New Ulm. The first run used a full year of discharge and chemistry data; the second removed nitrate concentration data for December, January, and February and changed discharge data for the same time period to 0.0028 m^3/s, which was two orders of magnitude lower than the minimum discharge value during this time period of 0.44 m^3/s. The first run represented the control, and the second run represented the results without winter nitrate or accurate discharge data.

Summaries of nitrate concentrations for April through October for the two runs are listed in Table A-4 of the Appendix. Note that the time period is offset by a month at the beginning and the end of the period during which nitrate and discharge data were altered, so that there was data available to be factored into the seasonal component of the regression equation even at the beginning and end of the season. As is evident from Table A-4, vastly incorrect discharge data for the winter season had little effect on nitrate concentration estimates for the rest of the year when nitrate concentration data was also removed from the winter season. The median annual difference between the two runs was only 0.09 mg/L, and the maximum difference was 0.19 mg/L. It is reasonable to assume that these differences are larger than the error in running the WRTDS model at Lamberton with estimated discharge from the regression relationships between Lamberton and New Ulm, since the estimated discharge was a better approximation than the 0.0028 m^3/s discharge used in the sensitivity analysis.

A final note on the data used in the WRTDS model is that occasionally, a few (i.e., 1 to 10) days of discharge data was missing from the record, presumably due to equipment failure. For these small gaps in data, linear interpolation between the two discharge values on either side of the gap was used to estimate the discharge values for these dates.

Any nitrate concentration data that was present during the gap in discharge data was removed, so that the interpolated discharge values would not affect the estimation of the coefficients in the regression equation.

4. Results

4.1. Water sampling and cation concentrations

Water sampling took place throughout the growing season of 2017. Figure 3 shows the hydrograph at the MN DNR's Lamberton gage station during the study, with stream sampling dates at the Lamberton sampling site (approximately 3 river miles upstream from the gage) indicated.

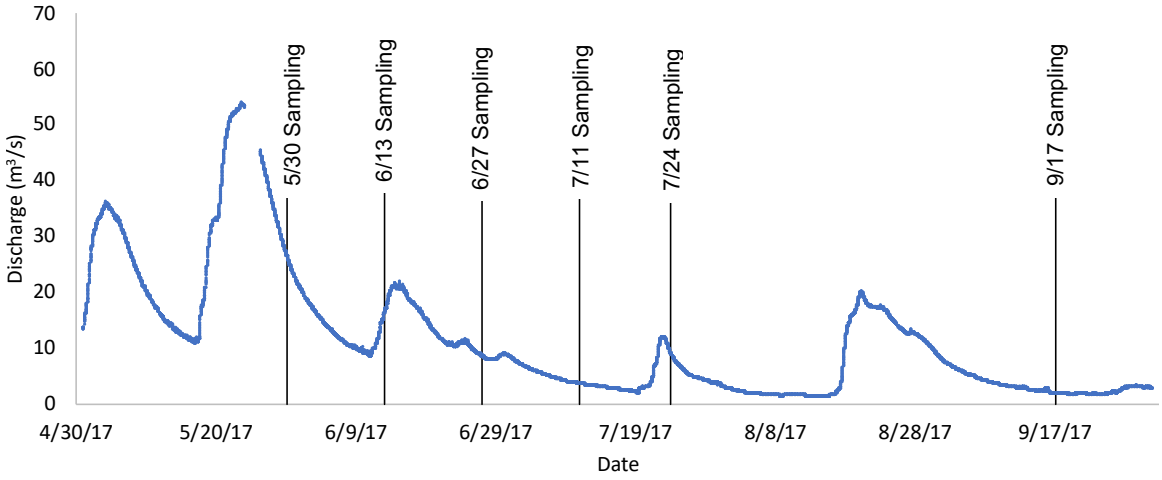

Figure 3. Cottonwood River hydrograph at Lamberton gage (MN DNR) with Lamberton stream sampling dates indicated.

Concentrations of all chemical constituents (except NO_{2+3}^{-}-N) measured in all water sources were plotted against each other to assess the possibility of conservative mixing. Conservative mixing, wherein chemical concentrations do not change due to reactions or biological uptake, is necessary for chemical constituents to effectively trace water sources. Conservative mixing by chemical constituents is implied, though not proven, by approximately linear relationships between chemical constituents. The chemical constituents selected as tracers were Ca^{2+}, Mg^{2+}, Na^{+}, and Si^{4+}. Bivariate plots of concentrations of these tracers in all possible end-members and in stream samples are shown in Figure 4. Although some bivariate plots (i.e., plots involving Si^{4+} concentrations) are not very linear, the expectation of a generally positive relationship

between tracer concentrations is confirmed. Lack of linearity in bivariate plots is likely due to differences in tracer ratios between water sources. Tracer concentrations varied between water sources sampled; medians and distributions of each tracer for each water source are summarized in Figure 5.

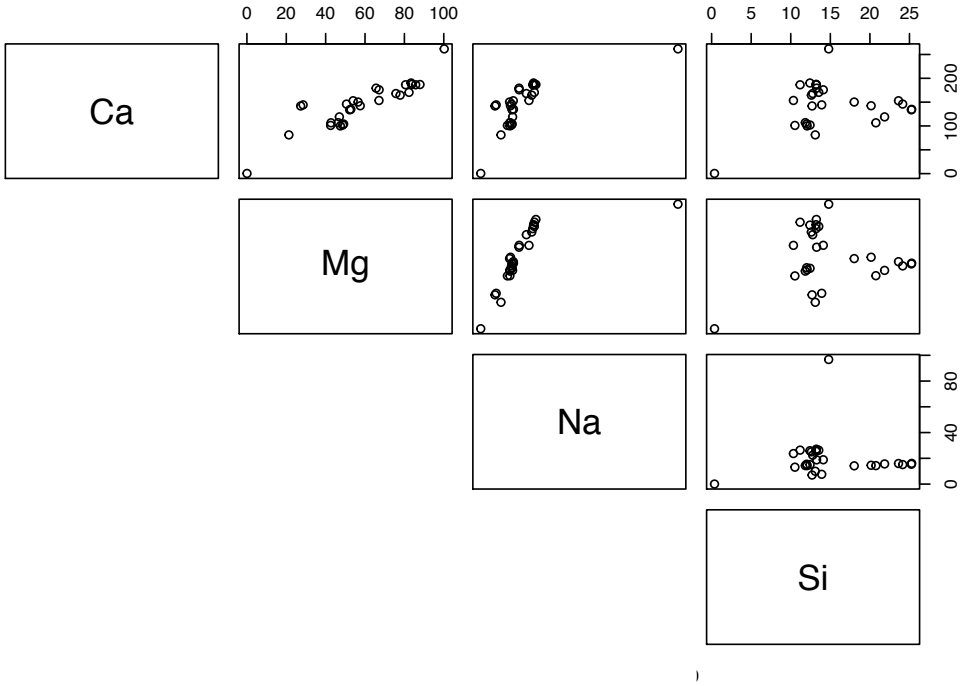

Figure 4. Bivariate plots of tracer concentrations in all possible end-member and stream samples used in EMMA (all units are mg/L).

Riparian groundwater sample collection followed two methods: purged sample collection and non-purged sample collection. For the farm riparian and prairie riparian PVC wells, the differences between purged and non-purged chemical results were large, and only data from the purged method was used. For the woods riparian well, purging made little difference for the constituents of interest. Specifically, the maximum difference in NO_{2+3}^{-}-N concentration was 0.1 mg/L, and the maximum percent difference for the cations selected as tracers for the EMMA (calculated as purged concentration minus non-purged concentration, divided by purged concentration) was 1.67% for Ca^{2+}, 2.56% for Mg^{2+}, 1.60% for Na^{+}, and 3.62% for Si^{4+}. Given these small differences between purged and non-purged results from the woods riparian well, samples that were not subjected to the purging methodology are used. The minimal difference in purged and

non-purged samples from this well is attributed to the fact that groundwater appeared to move quickly downslope through this riparian area. This was evident during the purging process, because even when three volumes of water were purged from the well, the well level did not decrease significantly.

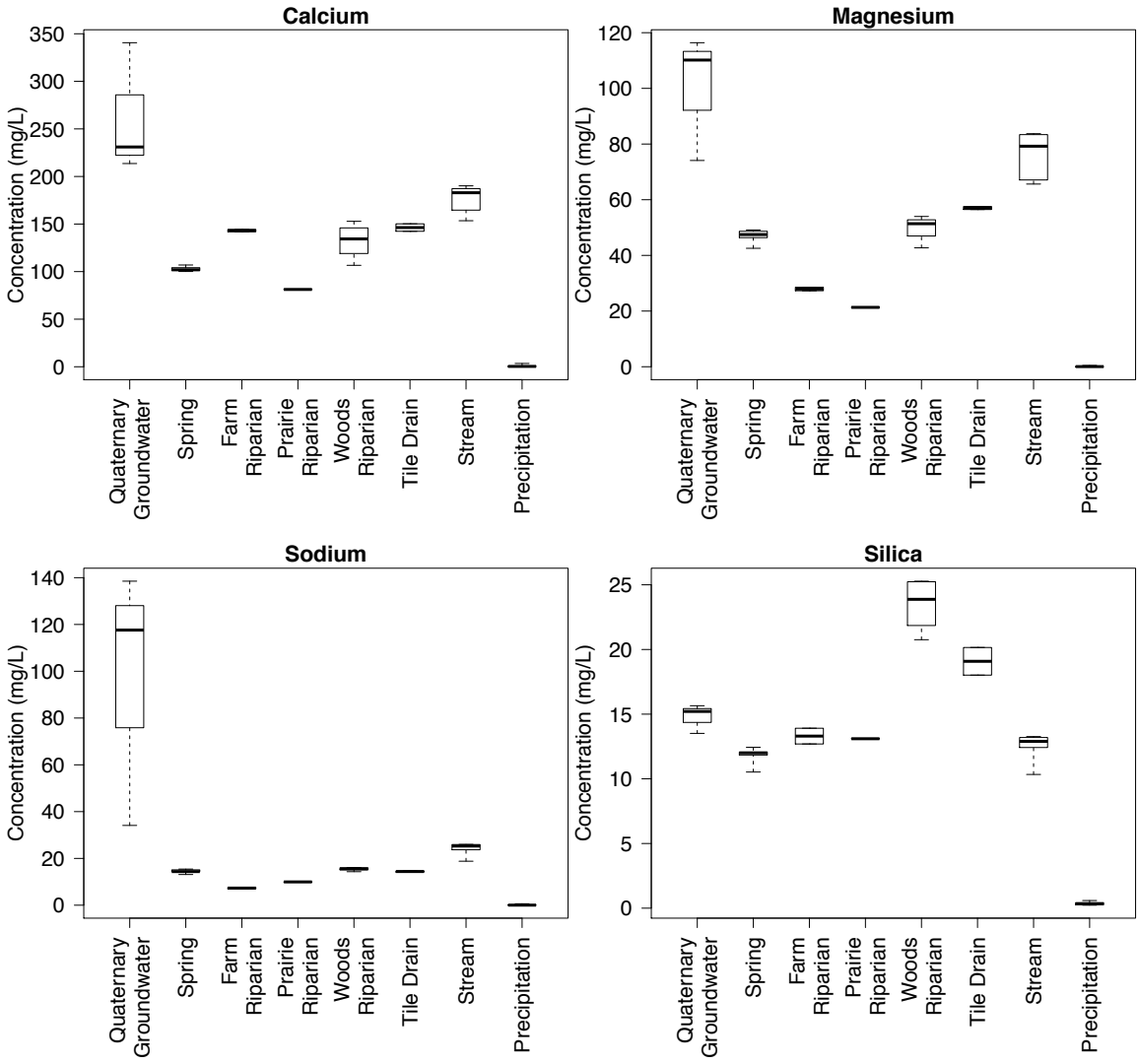

Figure 5. Box and whisker plots for tracer concentrations in possible end-members. Whiskers extend to maximum and minimum values; outliers are not identified. Sample sizes are as follows: Quaternary groundwater n = 3, spring n = 5, farm riparian n = 2, prairie riparian n = 1, woods riparian n = 6, tile drain n = 2, precipitation: median values from 373 weeks for calcium, magnesium, and sodium (NADP data); average values from 6 sites for silica (Anderson and Downing, 2006).

4.2. EMMA hydrograph separation results

When a principal components analysis was performed on the tracer concentrations from the six stream samples, it was found that the first two eigenvectors accounted for 95.3% of the variation in Ca^{2+}, Mg^{2+}, Na^{+}, and Si^{4+} concentrations. This indicates that two principal components and three end-members should be chosen. The possible end-members (tile drainage, spring, Quaternary groundwater, precipitation, prairie riparian, woods riparian, and farm riparian) were projected into the two-dimensional U-space defined by principal components one and two of the stream data. All water sources (stream samples and possible end-member samples) are plotted in this U-space in Figure 6.

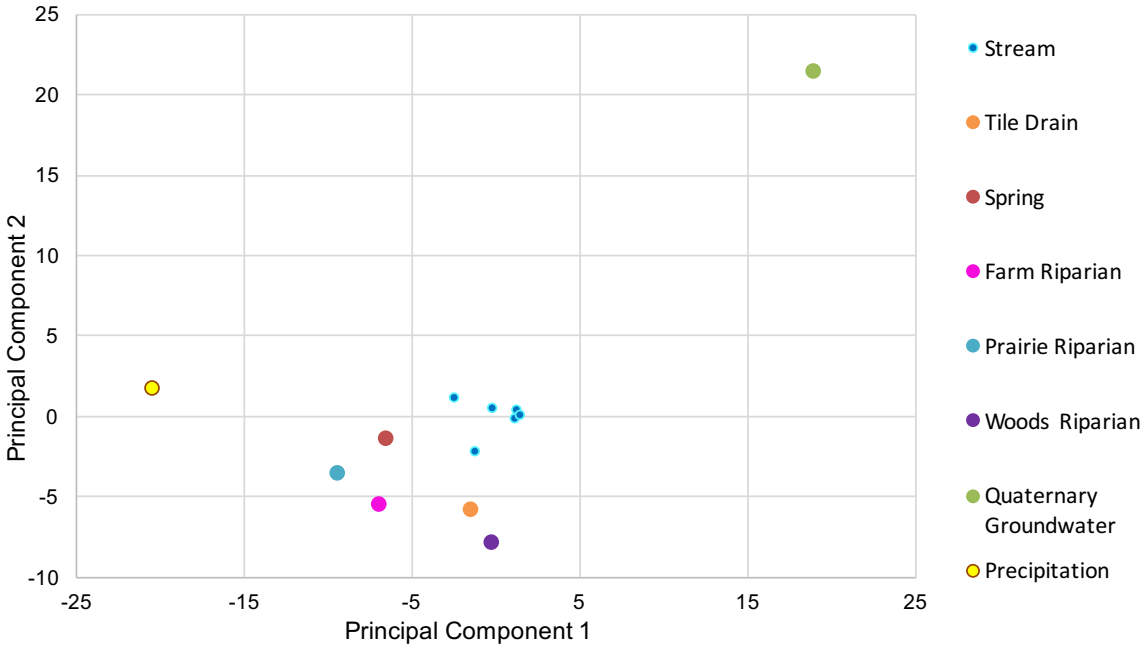

Figure 6. All possible end-members to stream water projected into the principal component space defined by stream.

Based on Figure 6, three end-members to the stream were selected. End-member selection followed two criteria. First, end-members were required to bound stream data. Second, priority was given to end-members that were closer to the plane defined by principal components one and two when plotted in the four-dimensional space defined by the four eigenvectors that resulted from the PCA. Based on these guidelines, Quaternary groundwater, spring, and tile drain were selected as the three end-members to the stream. Below, Figure 7 shows the stream data plotted with these three end-members only. End-

member error bars indicate the interquartile range in principal component one and principal component two, which represents variation from repeated sampling. For stream data points, standard deviation error bars are calculated from repeated analytical measurements on a single sample. Error bars that do not appear on the graph are within the size of the plotted data point.

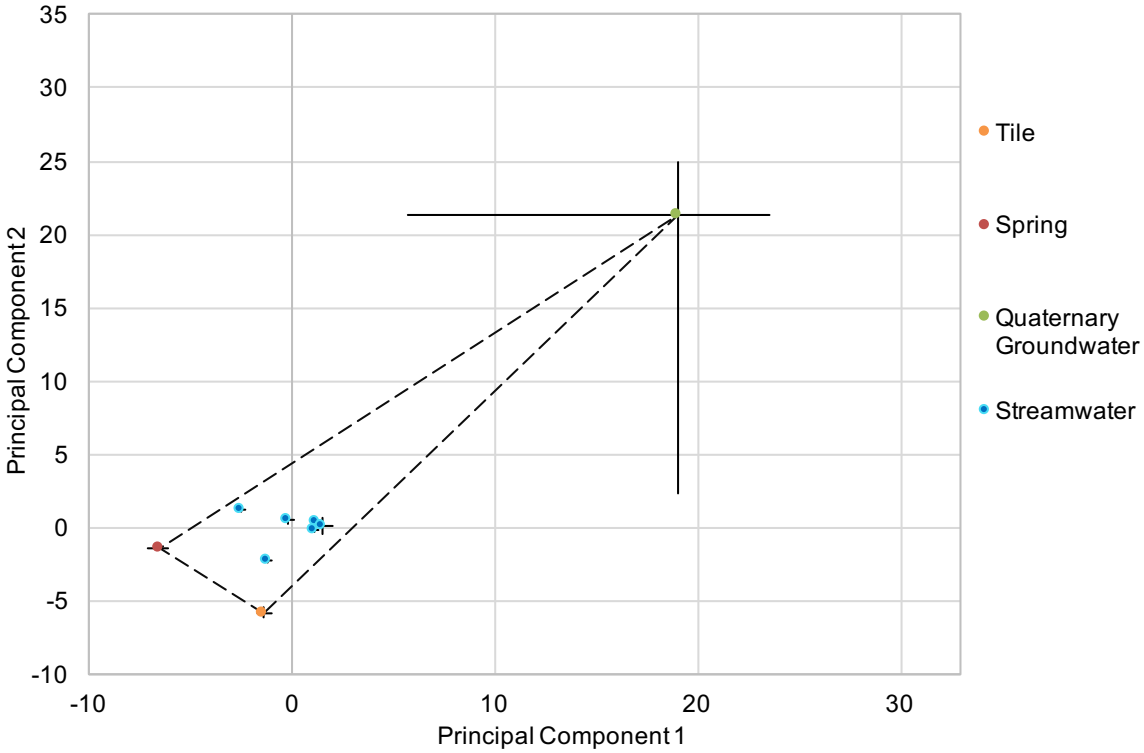

Figure 7. End-member mixing diagram for Cottonwood River at Lamberton.

Using tile drainage, spring water and Quaternary groundwater as end-members to the stream, percentages of each end-member contributing to the stream were calculated. The resulting contributions to the stream, expressed both as a percentage of streamflow and as volumetric discharge, are listed in Table 3. For most sampling dates, tile drainage composed the highest proportion of stream water and Quaternary groundwater composed the lowest. The volumetric discharge of Quaternary groundwater decreased notably over the course of the sampling season. Interquartile ranges for end-member contributions to streamflow (calculated using the 64 most extreme end-member contribution scenarios possible) are quite wide, mainly due to the large variability in the Quaternary groundwater end-member. These ranges are given in Table A-5 of the Appendix.

Table 3. Contributions of end-members to stream.

Sample Information		End-Member Percentages to Streamflow			End-Member Volumetric Discharges to Streamflow (m^3/s)		
Date	Discharge (m^3/s)	Tile	Spring	Quaternary Groundwater	Tile	Spring	Quaternary Groundwater
5/30/17	25.31	56.72%	24.41%	18.87%	14.36	6.18	4.78
6/13/17	18.08	61.53%	20.93%	17.54%	11.13	3.78	3.17
6/27/17	8.34	62.33%	19.04%	18.62%	5.20	1.59	1.55
7/11/17	3.64	41.58%	42.02%	16.40%	1.51	1.53	0.60
7/24/17	8.15	61.61%	29.90%	8.49%	5.02	2.44	0.69
9/17/17	1.89	10.84%	75.54%	13.62%	0.21	1.43	0.26

4.2.1. Observation well elevation data

Quaternary groundwater level is monitored by the MN DNR in observation wells in the area southwest of the study site at Lamberton, where Quaternary groundwater contributes to the Cottonwood River at Lamberton (Bradt 1997). Water elevations from two of these wells, which are in the Quaternary groundwater aquifer, were compared to the decrease in volumetric Quaternary groundwater discharge that was found by the EMMA chemical hydrograph separation (Figure 8). Decreases in well water elevation and Quaternary groundwater discharge to the stream have similar timing during the course of the summer.

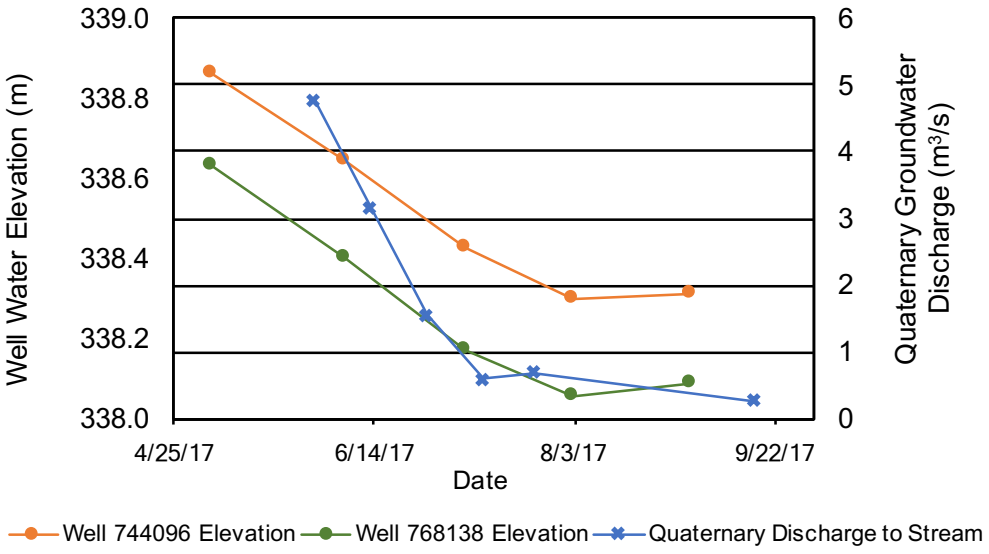

Figure 8. Comparison of decreases in well water table elevation (Quaternary groundwater wells) to decrease in Quaternary groundwater discharge in Cottonwood River at Lamberton.

4.2.2. Alternative hydrograph separation methods

A variety of methods to perform hydrograph separation using stream discharge data, including PART, the Lyne and Hollick digital filter, the Eckhardt digital filter, and Barne's method of graphical recession analysis were applied to the stream discharge record for the Cottonwood River at Lamberton. The results were compared to each other and to the EMMA chemical hydrograph separation results.

PART, the Lyne and Hollick digital filter, and the Eckhardt digital filter baseflow estimates during the 2016-2017 calendar year varied widely, especially during hydrograph peaks (Figure 9). PART typically yielded the highest estimate of baseflow and the Lyne and Hollick filter typically yielded the lowest estimate. When compared to EMMA chemical hydrograph separation results, estimates of baseflow from PART, the Lyne and Hollick digital filter, and the Eckhardt digital filter were all higher than the EMMA Quaternary groundwater component, as well as higher than the Quaternary groundwater component plus the spring groundwater component (Table 4).

Figure 10 shows the Barnes' method recession curves compared to PART, the Lyne and Hollick digital filter, the Eckhardt digital filter, and EMMA results where available (for one date) for five recession periods from 2016 to 2017 in the Cottonwood River at Lamberton. Four of the five recession periods display one recession curve; the fifth displays three. It is standard to refer to the separated components of the hydrograph using this method as baseflow, interflow, and surface runoff; however, such process-based interpretations will not be made here because sources such as tile drainage and shallow groundwater may not fit these categories well. Four of the recession curves had similar slopes (minimum of -0.0127 $m^3s^{-1}h^{-1}$, maximum of -0.0129 $m^3s^{-1}h^{-1}$). When compared to the other recession curves' slopes (-0.0333 $m^3s^{-1}h^{-1}$, -0.0044 $m^3s^{-1}h^{-1}$, and -0.0862 $m^3s^{-1}h^{-1}$), it seems probable that the four curves with slopes near -0.0128 $m^3s^{-1}h^{-1}$ represent recession of the same source of water. The other curves are interpreted to represent other sources of discharge to the stream that peak and recede with varying timing depending on the precipitation event characteristics, the discharge level, and the length of the recession period.

Baseflow estimates from PART, the Lyne and Hollick filter, and the Eckhardt filter are also plotted on the recession limbs (Figure 10). These three methods of hydrograph separation do not have a consistent relationship with the common recession curve that appears on four of the recession limbs. In other words, the PART, Lyne and Hollick, and Eckhardt baseflow estimates are above, near, or below the recession curve with slope of approximately -0.0128 $m^3s^{-1}h^{-1}$, depending on the recession period. This indicates that PART, Lyne and Hollick, and Eckhardt do not consistently track one particular discharge source to the stream (at least not during short-term recession periods).

For one recession period, chemical hydrograph separation data was also available. Quaternary groundwater, as determined by the chemical separation, was well below all estimates of baseflow; however, the sum of Quaternary groundwater and shallow groundwater was well aligned with one of the recession curves using the Barnes method (Figure 10).

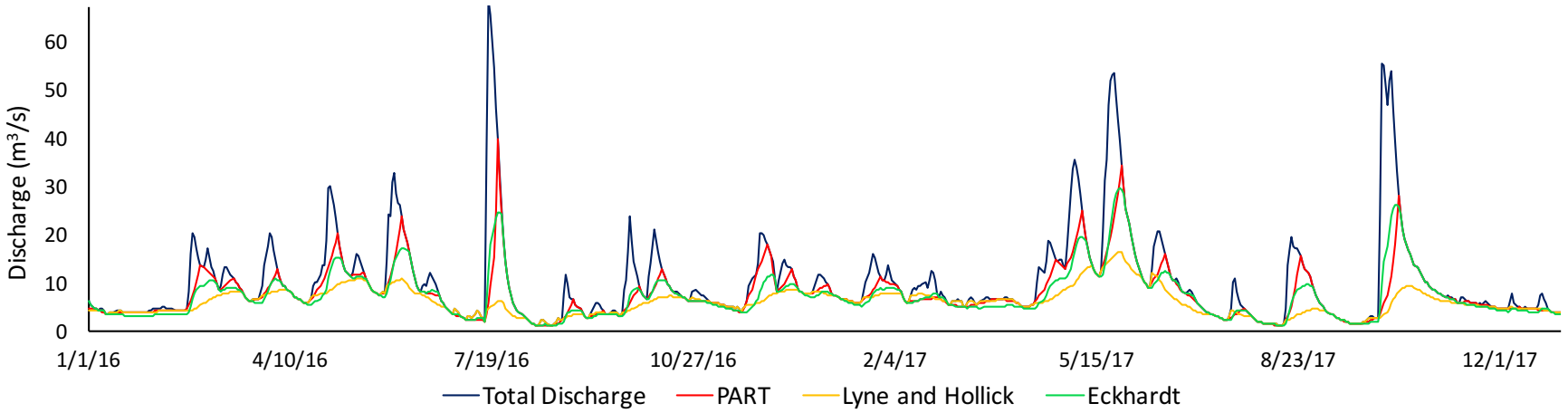

Figure 9. Comparison of PART, Lyne and Hollick digital filter, and Eckhardt digital filter in the Cottonwood River at Lamberton for 2016 through 2017.

Table 4. Comparison of chemical hydrograph separation, PART, Lyne and Hollick digital filter, and Eckhardt digital filter for 2016-2017.

Sample Information		**Chemical Separation End-Member Percentages**				**Alternative Hydrograph Separation Methods: Baseflow Percentages**		
Date	Discharge (m^3/s)	Tile	Spring	Quaternary Groundwater	Spring + Quaternary Groundwater	PART Baseflow	Lyne & Hollick Baseflow	Eckhardt Baseflow
5/30/17	25.31	56.72%	24.41%	18.87%	43.28%	100.00%	56.27%	100.00%
6/13/17	18.08	61.53%	20.93%	17.54%	38.47%	62.70%	67.56%	55.65%
6/27/17	8.34	62.33%	19.04%	18.62%	37.67%	100.00%	68.43%	100.00%
7/11/17	3.64	41.58%	42.02%	16.40%	58.42%	100.00%	100.00%	100.00%
7/24/17	8.15	61.61%	29.90%	8.49%	38.39%	45.60%	47.59%	52.75%
9/17/17	1.89	10.84%	75.54%	13.62%	89.16%	100.00%	100.00%	100.00%

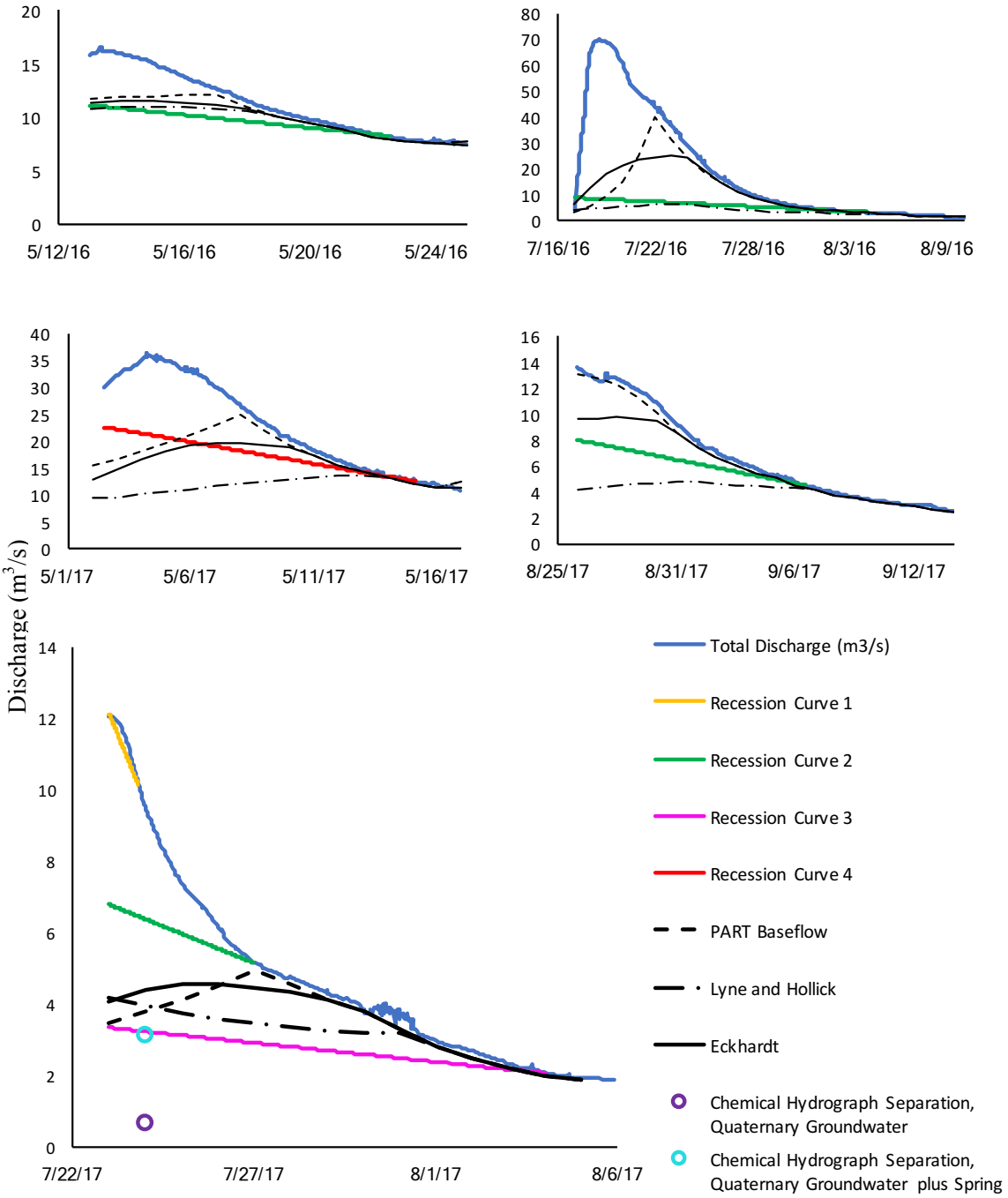

Figure 10. Comparison of various methods of baseflow separation. Recession curves determined by Barnes' method, baseflow determined by PART, Lyne and Hollick digital filter, and Eckhardt digital filter are displayed. Recession Curve 2, in green, has the same slope across the multiple recession periods during which it appears. Chemical hydrograph separation data from the EMMA is also displayed where available.

4.3. Nitrate mass balance results

Chemical concentrations of NO_{2+3}^--N were assumed to be composed almost entirely of nitrate (NO_{2+3}^--N), because it is expected that any nitrite present would be oxidized to nitrate. This expectation is confirmed by ion chromatography results from sampling on May 30, 2017 (ion chromatography analysis performed June 2, 2017). Results show maximum nitrite concentrations that range from below the detection limit to 0.08 mg/L. Therefore, NO_{2+3}^--N results will henceforth be treated as and referred to as nitrate (NO_3^--N).

The proportional contributions from each end-member to the stream, as well as measured nitrate concentrations from each end-member, were used to calculate an estimated nitrate concentration for the stream. This calculation used a weighted average technique under the assumption that nitrate behaved conservatively (an assumption that would subsequently be tested, as described below). The measured end-member nitrate concentrations used in this calculation are listed in Table 5. Monthly nitrate data were used for the tile drainage end-member because nitrate concentrations varied considerably over the course of the season. Spring water nitrate concentrations were consistent throughout the season (standard deviation of 0.66 mg/L), so the median of all samples collected was used in subsequent calculations. A median value for Quaternary groundwater was also used for all calculations.

Because nitrate is in high biological demand and undergoes many chemical transformations in aquatic systems (Delwiche 1970), it likely does not behave conservatively. Therefore, the calculated stream nitrate concentration was compared to the measured stream nitrate concentration from the same date. The calculated stream nitrate concentration was viewed as a prediction, and the measured stream nitrate concentration was used to elucidate processes for which the prediction did not account. Comparisons are expressed both as the difference between the predicted and the measured nitrate concentrations, and as a percentage of the predicted nitrate concentration that was not accounted for in the measured nitrate concentration (i.e., $1 - \frac{observed\ nitrate\ concentration}{predicted\ nitrate\ concentration} * 100\%$). This data is presented in Table 6. On five of the six sampling dates, observed nitrate concentration was less than predicted nitrate

concentration. The difference between observed and predicted nitrate concentration, henceforth called nitrate removal, ranged from 0.19 mg/L to 17.31 mg/L, or 1.91% to 94.54%. On the single date during which nitrate was added to stream rather than removed, only 1.11 mg/L (10.67% of incoming nitrate) was added.

Nitrate removal is presented in graphical formats (Figure 11, Figure 12, Figure 13, Figure 14) as both amount of nitrate removed (mg/L) and as percentage removal, and graphed versus both date and discharge in order to illustrate the relationships between nitrate removal and both season and discharge. Nitrate removal was highest during low flows and late in the season, two conditions that are often conflated in the climate of the study site. Error bars represent the interquartile range, as propagated from end-member error bars in Figure 7.

Table 5. Nitrate concentrations in end-members to Cottonwood River.

Median End-Member Nitrate Concentrations (mg/L)			
	Tile Drain	Spring	Quaternary Groundwater
May*	10.34	23.3	0.5
June*	8.87		
July	7.55		
Sept	5.9		

*Data previously collected (2006 to 2009).

Table 6. Nitrate concentrations (observed and predicted) and removal calculations.

Sample Information		End-Member Percentages to Streamflow			Nitrate Mass Balance Calculations			
Date	Discharge (m^3/s)	Tile	Spring	Quaternary Groundwater	Observed Stream Nitrate (mg/L)	Predicted Stream Nitrate (mg/L)	Nitrate Removal (mg/L)	Percent Nitrate Removal (%)
5/30/17	25.31	56.72%	24.41%	18.87%	10.57	11.65	1.08	9.26%
6/13/17	18.08	61.53%	20.93%	17.54%	11.53	10.42	-1.11	-10.67%
6/27/17	8.34	62.33%	19.04%	18.62%	9.87	10.06	0.19	1.91%
7/11/17	3.64	41.58%	42.02%	16.40%	5.30	13.01	7.71	59.27%
7/24/17	8.15	61.61%	29.90%	8.49%	7.15	11.66	4.51	38.69%
9/17/17	1.89	10.84%	75.54%	13.62%	1.00	18.31	17.31	94.54%

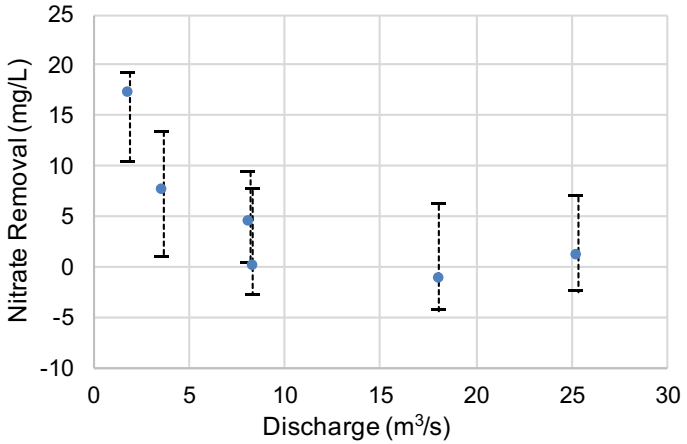

Figure 11. Discharge versus nitrate removal (as mg/L).

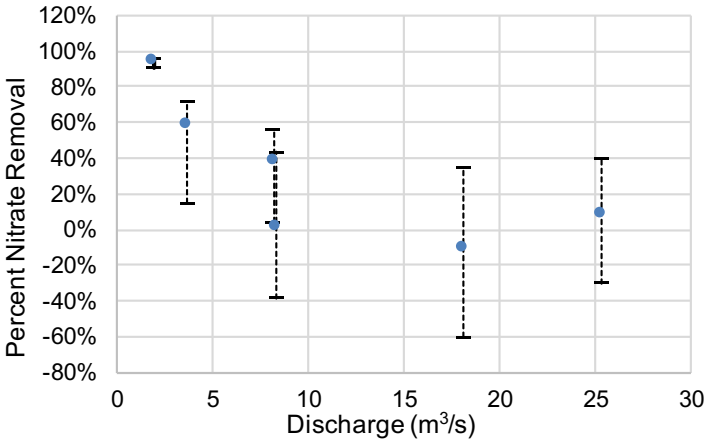

Figure 12. Discharge versus nitrate removal (as percentage).

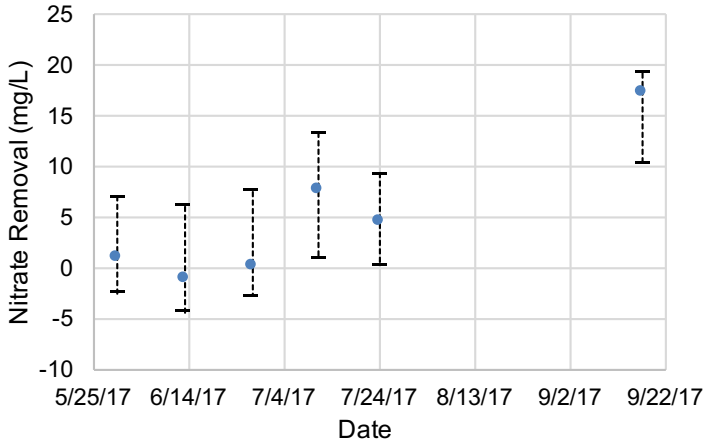

Figure 13. Date versus nitrate removal (as mg/L).

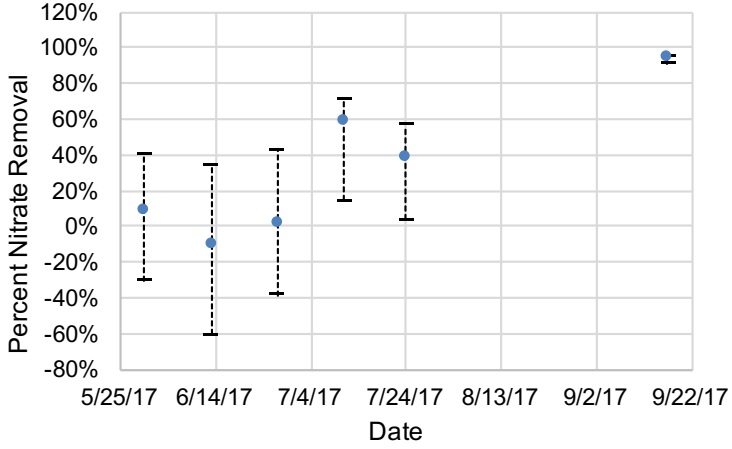

Figure 14. Date versus nitrate removal (as percentage).

4.4. WRTDS Model results

4.4.1. Model fit for Lamberton and New Ulm

The fit of the WRTDS model was assessed using plots that compared the measured nitrate data to the nitrate concentrations predicted by the WRTDS model (Figure 15 and Figure 16). Because the model uses a statistical smoothing approach, the phenomenon displayed in these figures where the modeled concentrations tends toward the center of the original data is expected.

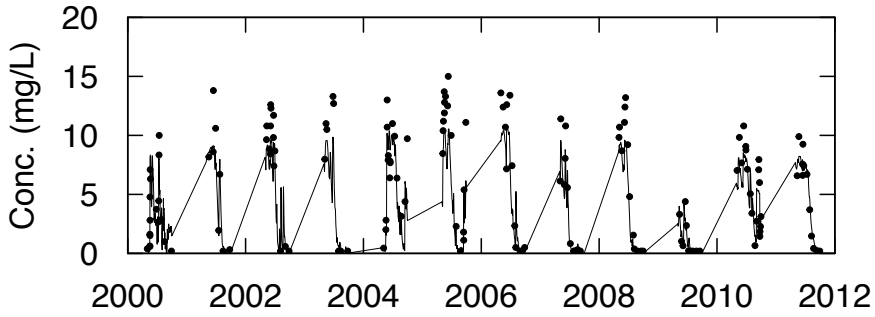

Figure 15. WRTDS model predictions of nitrate concentrations (solid line) compared to observed nitrate concentrations (dots) for Lamberton. Data are only for the time period during which data was available (April through September).

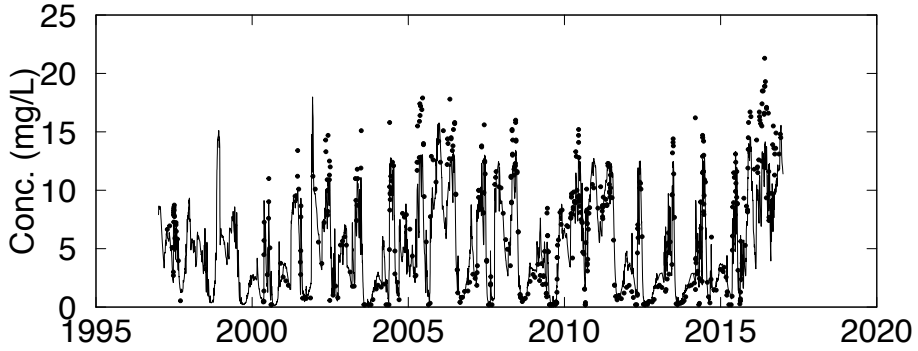

Figure 16. WRTDS model predictions of nitrate concentrations (solid line) compared to observed nitrate concentrations (dots) for New Ulm.

4.4.2. WRTDS concentration-discharge plots

Using the daily estimates for nitrate concentration generated by WRTDS, concentration-discharge plots were created. Data was segmented based on season, and a best fit line in the form of a second order polynomial was fit to each seasonal range. WRTDS estimates are plotted as individual data points for each seasonal range to show the distribution of discharge in the season (Figure 17 and Figure 18). Best fit lines are

also plotted on a single set of axes for comparison between seasons (Figure 19 and Figure 20). Lamberton concentration-discharge plots are found in Figure 17 and Figure 19. New Ulm concentration-discharge plots are found in Figure 18 and Figure 20.

Over low discharge levels, the second order polynomial best fit lines display a positive slope between discharge and nitrate concentration. For months during the growing season, the positive slope of the curves increases as discharge decreases; in other words, the best fit lines become steeper at lower flows. This effect is strongest for May through August in New Ulm, and is consistent throughout the seasonal range available (April through September) in Lamberton. The concentration-discharge curves also show a subtle decrease in nitrate concentration at very high discharges.

Examination of Figure 17 and Figure 18, in which the WRTDS-estimated concentration-discharge data are plotted, demonstrates that the distribution of concentration-discharge data varies seasonally. In general, discharge is lowest in September to October, and highest in May to June. This results in a seasonal pattern where nitrate concentrations are also lower in the fall and higher in the spring. The winter concentration-discharge data in New Ulm, however, do not adhere to this pattern; high nitrate concentrations are seen even at low discharges in the winter.

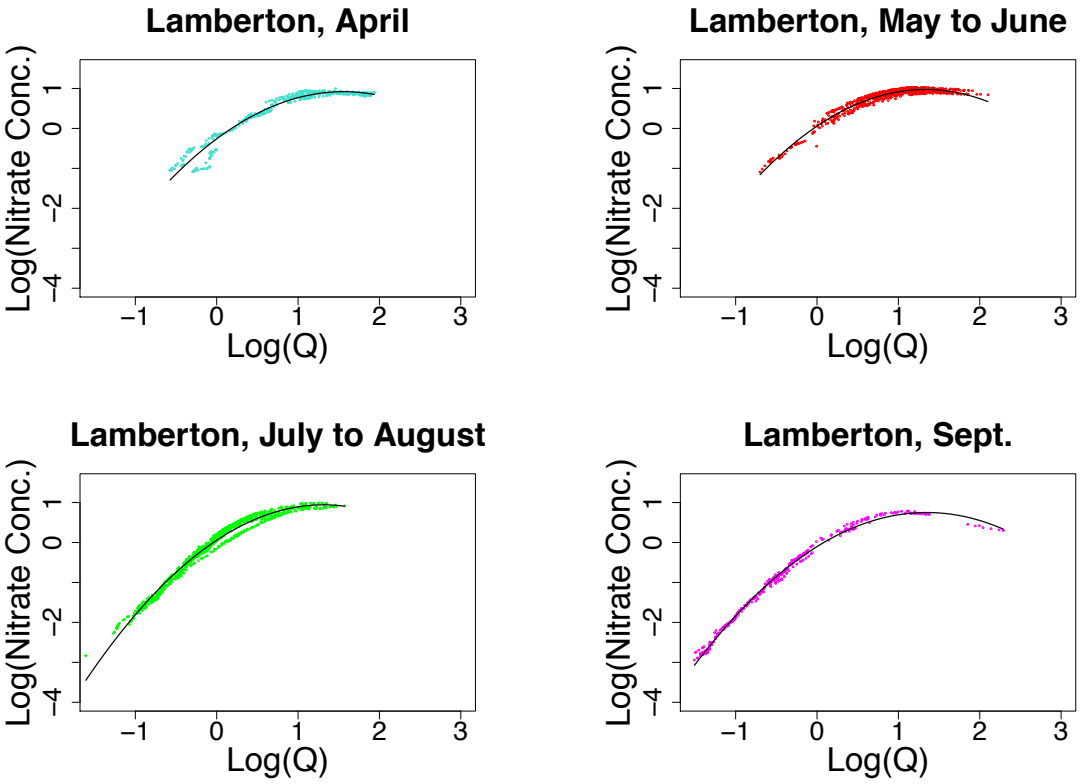

Figure 17. Concentration-discharge data for Lamberton, using WRTDS model nitrate concentration estimates. Black line is a 2nd order polynomial best fit line.

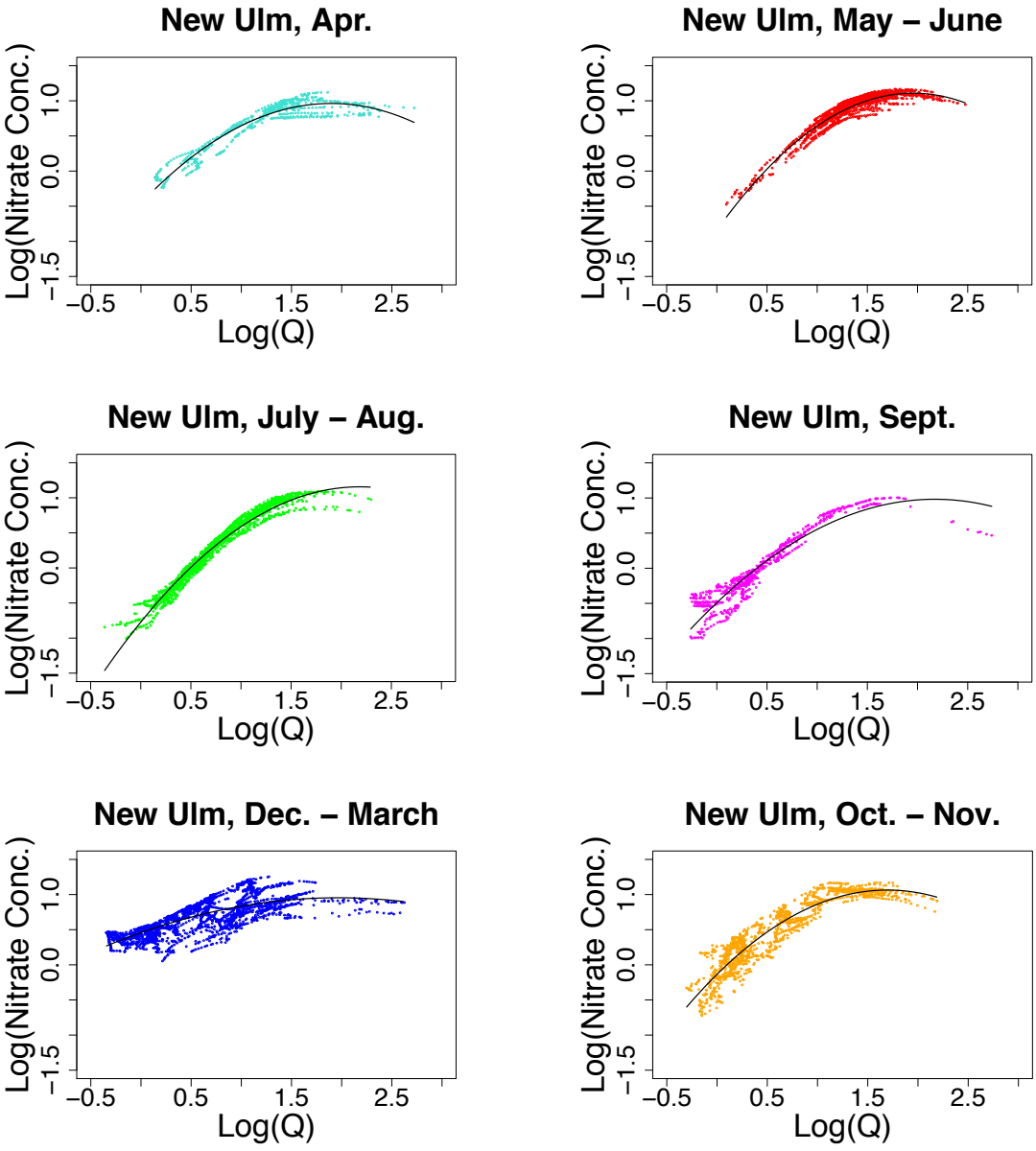

Figure 18. Concentration-discharge data for New Ulm, using WRTDS model nitrate concentration estimates. Black line is a 2nd order polynomial best fit line.

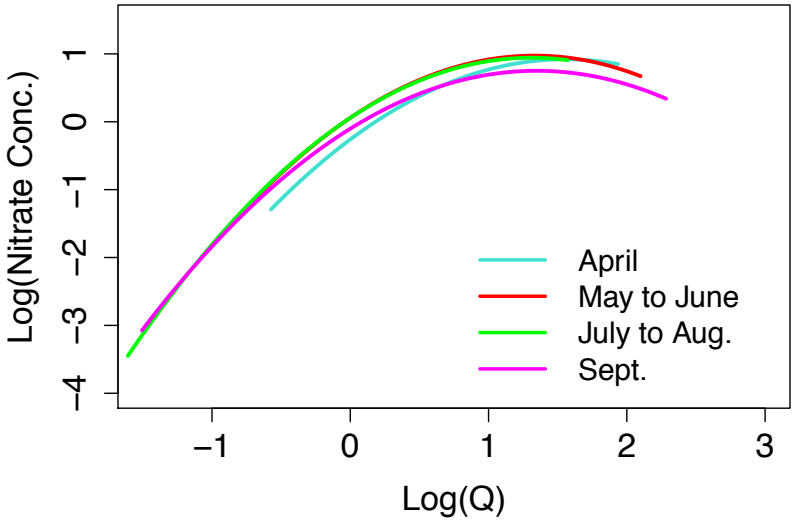

Figure 19. Concentration-discharge best fit lines for Lamberton, using WRTDS model nitrate concentration estimates. Best fit lines are 2nd order polynomial.

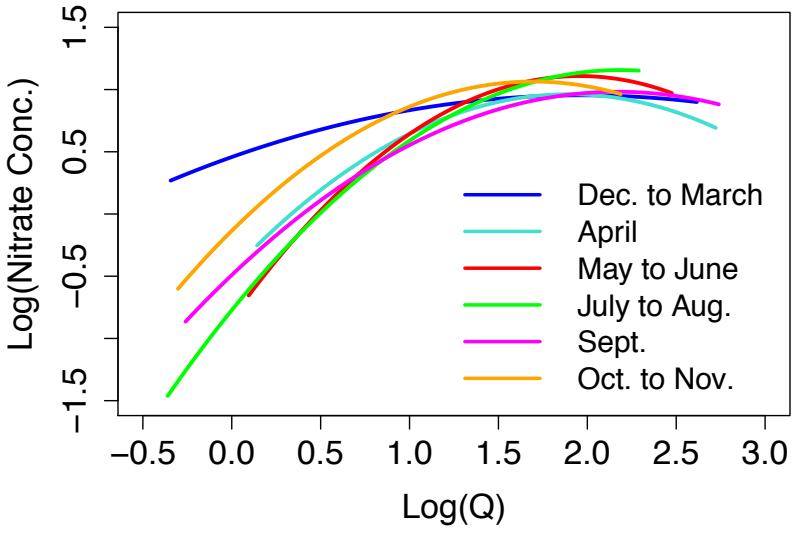

Figure 20. Concentration-discharge best fit lines for New Ulm, using WRTDS model nitrate concentration estimates. Best fit lines are 2nd order polynomial.

4.4.3. WRTDS nitrate time trend

The daily estimates of nitrate concentration data from the WRTDS model were also used to explore changes in nitrate concentrations over the time period modelled. This exploration was best suited to the New Ulm site, rather than the Lamberton site, due to New Ulm's longer (21 year) span of data on nitrate concentration and discharge. Figure 21 shows the modulations that nitrate concentrations have undergone in the Cottonwood River during this time period. Specifically, in the beginning of the study period, maximum winter nitrate concentrations were extremely high (between 15 and 20 mg/L), while maximum summer nitrate concentrations were below 10 mg/L. In contrast, more recent years have displayed a more consistent maximum nitrate concentration throughout the year of 10 to 15 mg/L.

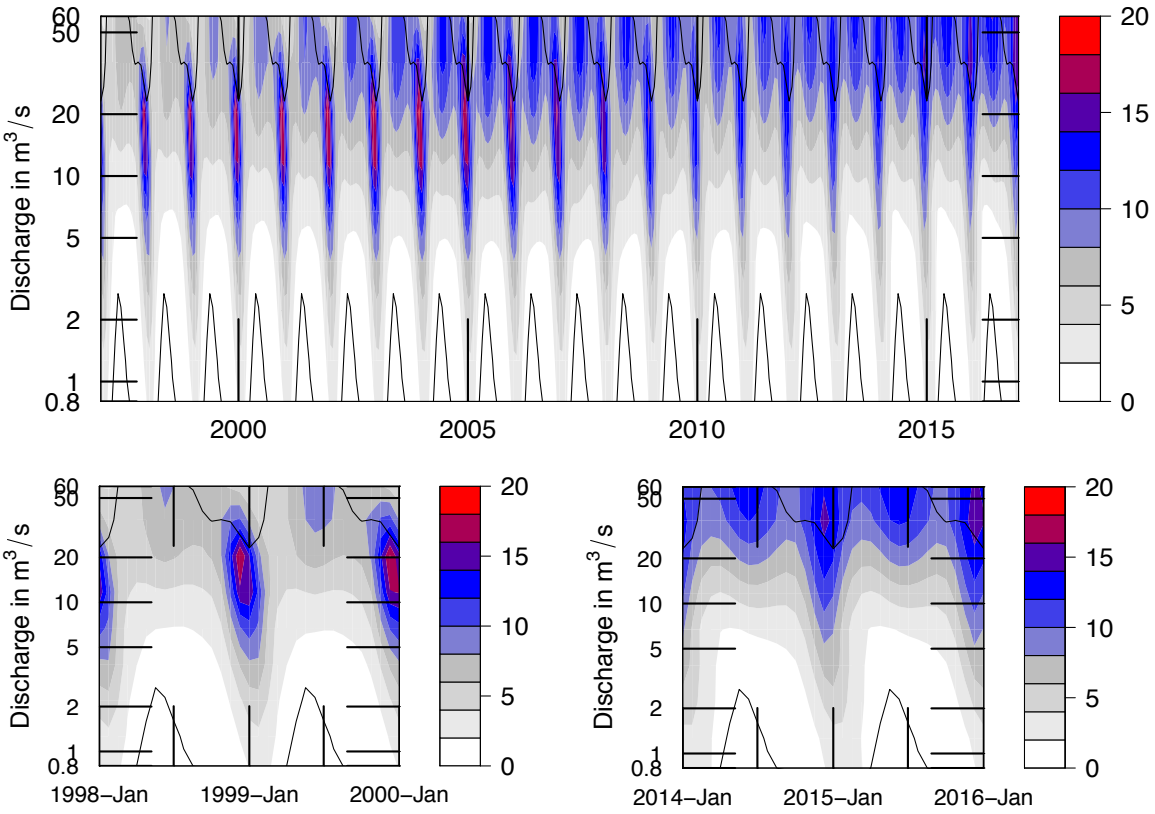

Figure 21. Contour plots of trends in New Ulm nitrate concentrations (in mg/L) from 1997 to 2017. Black lines denote 5th and 95th percentiles of discharge. Color key for nitrate concentrations in mg/L is shown on the left of each plot.

5. Discussion

5.1. Hydrograph separation

5.1.1. EMMA hydrograph separation

Hydrograph separation using EMMA demonstrated that stream flow in the Cottonwood River at Lamberton was mainly composed of tile drainage, spring water, and Quaternary groundwater (Table 3). The spring water is interpreted to be representative of shallow groundwater in the region, due to the spring's position in a hillside, its high nitrate concentrations (Table 5), and its perennial flow throughout the year.

Notably, riparian groundwater from three sites did not fit the criteria to be chosen as an end-member (Figure 6). This may seem contradictory given the proximity of riparian groundwater to stream water. However, the Cottonwood River at Lamberton has incised in its channel, thus reducing hydrologic connectivity between the stream and the riparian zone (Figure 22). This phenomenon is common in agricultural watersheds, and is attributed to increased channelization and straightening of streams (Potter, Douglas, and Brick 2004) as well as increases in overbank deposition due to flooding (Schilling, McLellan, and Bettis 2013). Channel incision creates a lower water table and a thicker unsaturated zone in the riparian area near the stream (Schilling, McLellan, and Bettis 2013). This decreases contact between groundwater and plant and microbial biogeochemical processes in the riparian zone, thus reducing the riparian zone's influence on chemistry in shallow groundwater, and in turn, on stream water.

Figure 22. Cottonwood River at Lamberton field site. Photo by Hilary Pierce.

For sampling dates between May and July, tile drainage was the largest, or near largest, contributor to stream flow (Table 3). Given the dominantly agricultural land-use in the watershed and the flat topography in the region near Lamberton, significant tile drainage contributions to the stream are reasonable. Hydrograph separation studies in agricultural settings have found that tile drainage can compose up to 54% of baseflow (Schilling et al. 2012), and up to 61% of overall watershed discharge (King, Fausey, and Williams 2014). These values are similar to the approximately 42% to 62% contribution of tile drainage to stream flow that was found in this study (Table 3). The September sampling date had significantly lower tile drainage contribution, which is explained by the minimal precipitation (3.0 cm) in the preceding four weeks ("Climate Data for Lamberton Southwest Research and Outreach Center" 2018).

Volumetric discharge from Quaternary groundwater decreased significantly over the course of the study (Table 3). Such a decrease was not expected, given the depth of the Quaternary aquifer. However, the lowest volumetric discharge of Quaternary groundwater to the stream found in this study, 0.26 m^3/s, matched well with the 10^{th} percentile of 7-day minimum stream discharge of 0.25 m^3/s, calculated using daily stream discharge data from 2013 to 2017. This indicates that such a discharge from Quaternary groundwater is not unreasonable. Furthermore, observation well data from the Quaternary aquifer in the region showed decreases of approximately 0.5 m from June 2017 to September 2017 (Figure 8). This decrease in groundwater storage corroborates the decreased volumetric discharge of Quaternary groundwater to the stream at the Lamberton field site during the same time period.

5.1.2. Alternative hydrograph separation methods

Hydrograph separations from PART, the Lyne and Hollick digital filter, the Eckhardt digital filter, graphical recession analysis and EMMA chemical hydrograph separation results gave wide-ranging estimates of baseflow. In general, baseflow estimates by PART were highest, followed by the Eckhardt digital filter and the Lyne and Hollick digital filter (Figure 9). Hydrograph separations by graphical recession analysis (Barnes 1940) did not have a consistent relationship with any of those three methods (Figure 10). PART, the Lyne and Hollick digital filter, and the Eckhardt digital filter all gave higher baseflow

contributions to the stream than the contributions of Quaternary groundwater plus shallow spring groundwater as calculated using the EMMA (Table 4).

Previous studies have also compared these methods of hydrograph separation to each other. For a variety of watersheds in Australia, it was found that the Lyne and Hollick filter (with alpha of 0.925) estimated a higher baseflow than chemical hydrograph separation (Ladson et al. 2013), similar to this study's results (Table 4). Another study determined that PART provides higher baseflow indices for a variety of catchments than does the Lyne and Hollick filter (Arnold et al. 1995), which is again in agreement with this study's results (Figure 9). When applied to 65 watersheds in North America, PART and Eckhardt provided similar mean baseflow indices, which aligns with the similarity between this study's PART and Eckhardt results (Figure 9). Studies such as the aforementioned two that compare PART, Eckhardt, and Lyne and Hollick results to each other are only speculative in nature, however, because it is difficult to say which method provides the correct answer without chemical hydrograph separation.

A previous study that combined PART and other baseflow separation methods with field data found that tile drainage contributed to baseflow according to PART (Schilling and Helmers 2008). If the Lyne and Hollick and Eckhardt methods treat tile drainage similarly, this may explain the lack of similarity between these methods and the EMMA chemical hydrograph separation results. Specifically, all three components of the hydrograph as identified by the chemical hydrograph separation may be categorized (partly or wholly) as baseflow by PART, Lyne and Hollick, and Eckhardt, thus yielding the high baseflow indices by these methods seen in Table 4.

The variety in slopes of Barnes' recession curves in Figure 10 underscores the complexity of discharge sources that may contribute to the stream. In this setting, such sources may include surface runoff, tile drainage, soil water, shallow groundwater, and deep (i.e., Quaternary) groundwater. Because each source recedes at a different rate, the goal of categorizing streamflow into two distinct categories of baseflow and quickflow may be overly simplistic (Nathan and McMahon 1990). PART, Lyne and Hollick, and Eckhardt, all of which split the hydrograph into only two components, may not align with

recession curve and chemical hydrograph separation results because the latter methods allow for a more complex representation of water sources.

Despite the oversimplication inherent in the baseflow versus quickflow paradigm, digital filters have potential to provide useful information when calibrated using chemical hydrograph separation results. In a previous study, the Eckhardt digital filter was calibrated to chemical hydrograph separation results from a conductivity mass balance by adjusting the maximum baseflow index and alpha parameters in the filter (Zhang et al. 2013). This approach yielded a close fit between the digital filter separation and the conductivity separation (Zhang et al. 2013). Similar techniques have been employed by Ladson et al. (2013) using the Lyne and Hollick filter and Gonzales et al. (2009) using the Eckhardt filter. If a close fit between chemical hydrograph separation and digital filter separation can be achieved, it would enable accurate hydrograph separation to be performed during time periods for which only discharge data, not chemical data, are available (Gonzales et al. 2009; Zhang et al. 2013). No attempt to calibrate digital filters with chemical hydrograph separation results was made in this study because of the limited temporal range of chemical hydrograph results. However, if this constraint did not exist, calibration of a digital filter could enable long-term hydrograph separation, thus deepening the understanding of the relationships between water sources, discharge level, and in-stream nitrate concentration (using available long-term stream nitrate data).

5.2. Nitrate removal

5.2.1. Possible nitrate removal processes

On five of the six sampling dates, predicted nitrate was higher than observed nitrate (Table 6). This difference is attributed to removal of nitrate via in-stream biogeochemical processes. Higher measured than predicted nitrate concentration on the remaining sampling event could be due to either a source of water and nitrate that was not accounted for in the EMMA, or to nitrification (nitrate production) within the stream.

Typically, in-stream nitrate removal has been credited to microbial or plant uptake of nitrate, and denitrification (Burgin and Hamilton 2007). Many studies assume that these two processes are the most likely causes of nitrate removal without providing site-specific justification (e.g., Mulholland et al. 2008; Peterson et al. 2001). Plant and

microbial uptake of nitrate does not truly remove nitrate from the system, because when plants senesce and decompose they release the nitrate back to the environment (Ranalli and Macalady 2010). Denitrification is defined as the reduction of nitrate that occurs when nitrate is used as the terminal electron acceptor by microbes oxidizing organic matter (Seitzinger et al. 2006). Bacteria perform denitrification facultatively in order to respire in an anaerobic environment, though they are also capable of aerobic respiration (Seitzinger et al. 2006). Complete denitrification results in the production of dinitrogen gas (N_2) that is released to the atmosphere (Ranalli and Macalady 2010), while incomplete denitrification releases N_2O or NO gases to the atmosphere (Matson, Lohse, and Hall 2002). Both complete and incomplete denitrification are permanent removal pathways for nitrate from the stream environment. In a meta-analysis of denitrification rates in aquatic environments, it was found that high denitrification rates occur in dark environments, conditions with little plant growth, low total phosphorus, low dissolved oxygen, high nitrate concentrations, and high organic carbon concentrations (Piña-Ochoa and Álvarez-Cobelas 2006). Furthermore, denitrification is promoted at boundaries between oxic and sub-oxic environments (Seitzinger et al. 2006). For instance, sub-oxic aquatic sediments beneath oxic water provide an oxygen gradient that promotes denitrification of nitrate that enters the sediments from the water (Seitzinger et al. 2006).

Another process that could remove nitrate from the Cottonwood River at Lamberton is dissimilatory nitrate reduction to ammonium (DNRA) (Burgin and Hamilton 2007). DNRA is the reduction of nitrate to produce ammonium (Rütting et al. 2011). The ammonium produced by DNRA may be taken up by plants and microbes, or nitrified back to nitrate (Burgin and Hamilton 2007). Although DNRA is significantly less studied than denitrification, it can be executed by a variety of soil bacteria and fungi (Rütting et al. 2011). Similar to denitrification, DNRA also requires a low-oxygen environment (Rütting et al. 2011). Theoretically, denitrification produces more free energy than DNRA and should therefore be advantageous to organisms over DNRA, but results from lab experiments have shown denitrification yielding less free energy than DNRA (Rütting et al. 2011). Furthermore, nitrate is able to accept more electrons in DNRA than in

denitrification, so in settings where electron acceptor availability is limited, DNRA may be preferred by organisms over denitrification (Rütting et al. 2011).

This study did not attempt to specify which of these processes removed nitrate from the stream water. However, few to no aquatic plants grow in the Cottonwood River at or upstream of the Lamberton field site (Figure 22), so it seems reasonable to assume that plant uptake of nitrate is not a major cause of nitrate removal in this study. A study in another agricultural setting in the upper Mississippi River Basin used the stable isotope of nitrogen, ^{15}N, to identify processes of in-stream nitrate removal and found that denitrification accounted for the majority of nitrate removal (Böhlke, Harvey, and Voytek 2004). This indicates that denitrification likely plays a role in nitrate removal in this study site. Nevertheless, DNRA and microbial uptake of nitrate are also plausible mechanisms for in-stream nitrate removal. Therefore, the study will henceforth refer to all processes that remove nitrate from stream water using the general term "nitrate removal."

5.2.2. Comparison of nitrate removal to previous studies

This study's finding that, on most sampling dates, nitrate was removed from the in-stream environment aligns well with previous work. Data from field studies that could be directly compared to this study's results are summarized below.

In an agricultural setting in Ontario, nitrate removal in the hyporheic zone of a stream was investigated using hydraulic gradient measurements as well as measurements of nitrate relative to chloride and injected bromide (Hill, Labadia, and Sanmugadas 1998). It was concluded that the hyporheic zone was a sink for nitrate, and attributed this behavior to the high concentration of nitrate in the watershed due to agricultural land use (Hill, Labadia, and Sanmugadas 1998). The present study also took place in an agricultural setting, and abundant nitrate in the watershed may have a similar effect on in-stream nitrate transformation.

A study with a very similar methodological approach to the one presented here was performed in a Mediterranean stream (Bernal, Butturini, and Sabater 2006). In it, EMMA was used to identify end-members to the stream, end-members were used to predict nitrate concentration, and this prediction was compared to measured stream nitrate concentrations. It was found that below a threshold discharge, nitrate was removed from

the stream, and above the threshold, nitrate was added to the stream (Bernal, Butturini, and Sabater 2006). The finding that lower discharge promotes nitrate removal aligns with the results of the present study.

Valett et al. (1996) also found that hyporheic zones acted as net sinks of nitrate, even in settings that were lithologically diverse. This study used solute-injection experiments to examine nitrate removal at three different sites with diverse bedrock in New Mexico (Valett, Morrice, and Dahm 1996). In all three sites, the hyporheic zone was a sink for nitrate, and almost half of the injected nitrate was removed from the hyporheic water; this significant removal of nitrate by in-stream processes corroborates the present study's findings. The hyporheic zones' slow flows and low oxygen concentrations were thought to cause nitrate removal (Valett, Morrice, and Dahm 1996).

Finally, nitrate removal in the hyporheic zone was examined using cores from a sandy streambed in Virginia (Gu et al. 2007). Nitrate-rich water was pumped through cores in a lab setting, and it was found that 80% of the nitrate in the water pumped into the core was removed by the core (Gu et al. 2007). This high level of nitrate removal helps to validate the highest removal of nitrate (94.54%) found by the present study.

5.2.3. Controls on nitrate removal in the hyporheic zone

Nitrate removal appeared to be promoted by the low discharge levels that occurred in the late summer and early fall in this study (Table 6). Previous research shows that the timing and magnitude of nitrate removal in the hyporheic zone can be explained by a variety of factors, all of which hinge upon the necessity for stream water to be in sufficient contact with the hyporheic zone for biogeochemical uptake processes of nitrate to occur. Contact between the hyporheic zone and stream water can be either spatial or temporal.

Spatially, stream water contact with the hyporheic zone is determined by the size and shape of the stream (i.e., the hydraulic radius). In a study of the Mississippi River Basin, it was found that smaller streams removed more nitrate than larger streams (Alexander, Smith, and Schwarz 2000). This difference was attributed to decreased interaction between the benthic sediment and the stream water in larger and deeper streams (Alexander, Smith, and Schwarz 2000). Another study that utilized a stream transport

model also found that water depth was an important predictor of denitrification, even for two watersheds with different nitrate concentrations (Alexander et al. 2009). A review of in-stream nitrate removal also indicated that decreased water depth promotes nitrate removal (Ranalli and Macalady 2010).

Temporally, stream water contact with the hyporheic zone is controlled by residence time of the stream water in hyporheic zone flow pathways. The ratio of water transport time to biogeochemical reaction time, called the Damkohler number, is a metric that quantifies whether the residence time is sufficient for biogeochemical uptake of nitrate (Zarnetske et al. 2012; Harvey et al. 2013). When the Damkohler number is greater than 1, water stays in contact with the streambed long enough for net denitrification to occur, according to modeling efforts (Zarnetske et al. 2012). Other studies have also supported the notion that residence time is critical for nitrate removal through field investigations in a variety of settings (Briggs, Lautz, and Hare 2014; Zarnetske et al. 2011; Harvey et al. 2013) and modeling (Boano et al. 2010). Residence time is controlled by a variety of factors, including hydraulic conductivity, geomorphology, stream velocity, and discharge levels. Some studies have directly correlated river discharge level to nitrate removal, finding that increased discharge leads to decreased removal of nitrate (Valett, Morrice, and Dahm 1996; Alexander et al. 2009). These findings support this study's result that more nitrate is removed at lower discharge levels. Decreases in discharge in the Cottonwood River at Lamberton increased water residence time, which in turn increased nitrate removal.

5.3. WRTDS model usage

5.3.1. Concentration-discharge analysis

WRTDS model results for daily nitrate concentration at Lamberton and New Ulm were used to create concentration-discharge plots for both sites (Figure 17, Figure 18, Figure 19, Figure 20). Using WRTDS model results is advantageous over using raw data for concentration-discharge analysis because the model results broaden the range of dates that are incorporated into the plot. Therefore, WRTDS model results remove any biases from the raw sampling data that might occur due to a disproportionate number of sampling dates at low or high discharges (Hirsch, Moyer, and Archfield 2010).

Furthermore, WRTDS model results increase the number of concentration-discharge pairs that can be plotted, thus reinforcing relationships in the raw concentration-discharge plots.

The second order polynomial best fit lines that relate discharge to nitrate concentration have a positive slope over low to moderate discharge levels, indicating that an increase in discharge results in an increase in nitrate concentration (Figure 17, Figure 18, Figure 19, Figure 20). This means that nitrate is transport-limited. Transport-limited behavior of nitrate in agricultural settings has been attributed to the build-up of nitrate in the soil throughout the watershed, which has resulted from heavy fertilizer use for many years (Basu et al. 2010). The stores of legacy nitrate enable in-stream nitrate concentrations to increase as the contributing area to the stream and the discharge increase.

Best fit lines display steeper positive slopes at low discharge levels during the growing season. The steepening slope of the concentration-discharge curve at low discharge indicates that nitrate is removed at a progressively higher rate with progressively lower discharge. This relationship has been interpreted to indicate that biogeochemical processes (such as nitrate uptake and denitrification) have a disproportionate effect on in-stream nitrate concentration at lower discharges compared to high discharges (Moatar et al. 2017). This pattern in concentration-discharge best fit lines does not describe the concentration-discharge relationship in New Ulm during winter months, however. During the winter, even low discharges often show very high nitrate concentrations, resulting in a more constant and less positive slope over the range of discharge (Figure 18, Figure 20). This can be attributed to the lack of biogeochemical processing of nitrate in the winter, and it supports the inference that more positive slopes at low discharge levels are due to biogeochemical uptake of nitrate. By the same logic, months with more severe increases in slope at low discharges have heightened biogeochemical removal of nitrate.

The slight decrease in nitrate concentration at very high discharges seen in the best fit lines can be interpreted as the result of a dilution effect. This effect could be caused by a decoupling of the sources of nitrate and water. For instance, perhaps at very high discharge levels, more of the discharge contributing to the stream comes from overland flow and therefore does not have the opportunity to transport nitrate stored in soils to the stream (e.g. Green et al. 2007).

Best fit lines for concentration-discharge relationships during the growing season (i.e., April to November) align well with each other for both the Lamberton and the New Ulm sites (Figure 19, Figure 20). However, seasonal differences in discharge mean that nitrate concentration varies seasonally. Specifically, discharge is typically lowest in September and highest in May to June (Figure 17, Figure 18). Therefore, it follows that nitrate concentrations are also generally lowest in September and highest in May to June.

5.3.2. Changes in nitrate concentrations through time

The WRTDS model is ideal not only for augmenting concentration-discharge data, but also for examining how concentration-discharge dynamics have changed during the study period. Application of this type of analysis to the Cottonwood River at New Ulm shows that nitrate concentrations have become more consistent throughout the seasons in the last 21 years (Figure 21). More constant nitrate concentrations in agricultural watersheds throughout the year have been attributed to increased tile drainage and the legacy build-up of nitrate in agricultural watersheds (Basu, Thompson, and Rao 2011). Surveys of tile drainage extent in minor agricultural watersheds in southern Minnesota revealed that between 1991 and 2010, the linear distances (lengths) of tile lines installed increased by 89.07% to 196.46%, depending on the watershed ("Tile Monitoring Project: Tile Reinventory"). Tile lines allow drainage water to bypass many of the biogeochemical processes that remove nitrate before water reaches the stream (Puckett 2004). It is thought that tile lines, as well as other agricultural engineering practices, are creating watersheds that display more constant processes throughout the year (Basu, Thompson, and Rao 2011).

The trend of increasing seasonal consistency in nitrate concentrations marks a departure from the patterns identified by this study of high nitrate removal during the

growing season and low nitrate removal during the winter (Figure 20). Given that seasonal nitrate removal patterns are likely biogeochemically mediated, it seems that increased tile drainage and anthropogenic interferences are beginning to override the natural nitrate processing dynamics in the watershed that this study documents.

5.4. Summary of implications for nitrate dynamics

The two approaches to examining in-stream nitrate removal in this study, the EMMA nitrate mass balance and the WRTDS concentration-discharge plots, corroborate each other convincingly. Both methods reveal that nitrate removal from the in-stream environment is highest at low discharges, which typically occur late in the growing season (i.e., September). The EMMA method examines sources of nitrate to the stream and nitrate removal amounts with a high level of detail, but only for a limited number of sampling dates over one season, in one location. The concentration-discharge analysis using WRTDS model results, on the other hand, utilizes data from many more sampling dates over a longer duration, in two locations in the watershed. The concentration-discharge analysis, therefore, gives more context to nitrate dynamics in the watershed and verifies that the EMMA nitrate mass balance results are representative of a broader pattern of increased nitrate removal at low discharges.

Watersheds in southern Minnesota are experiencing increased discharge due to changes in climate and land use (Novotny and Stefan 2007; Tomer and Schilling 2009; Schottler et al. 2014). This has important implications for nitrate concentration and export. Firstly, increased discharge will increase nitrate loads delivered to the watershed outlet, since nitrate is transport limited in this setting (Basu et al. 2010). Secondly, increases in discharge will also reduce in-stream nitrate removal via biogeochemical processes, since this study and others have shown that nitrate removal is highest at low discharges. These two effects will compound upon each other to worsen nitrate pollution in the Cottonwood River Watershed and in other similar settings (Raymond, David, and Saiers 2012).

5.5. Assumptions and future steps

5.5.1. EMMA assumptions

The results of the EMMA hydrograph separation rely on a series of assumptions about the water sources sampled and the watershed dynamics. The tracers used (Ca^{2+}, Mg^{2+}, Na^{+} and Si^{4+}) must act conservatively, meaning that their concentrations must not change due to biogeochemical processes or other reactions (Inamdar 2011). Further, tracer concentrations must be constant both spatially (throughout the watershed) and temporally (between sampling dates) (Inamdar 2011). In this study, it was assumed that the concentrations of tracers sampled at the tile drain, the three Quaternary groundwater wells, and the shallow groundwater spring are representative of those respective water sources in the watershed upstream of the Cottonwood at Lamberton. Additionally, the mixing of water sources and the resultant tracer concentrations must be assumed to be linear (Inamdar 2011).

5.5.2. Recommendations for future research

The assumptions described above should be verified by sampling from a broader selection of tile drains, Quaternary groundwater wells, and shallow groundwater sources. Increasing the spatial extent of end-member sampling would more accurately portray the end-members' chemistry in the EMMA hydrograph separation and the nitrate mass balance, thus increasing the certainty of those results. Furthermore, sampling at multiple locations along the Cottonwood River longitudinally could elucidate the ways in which water sources, nitrate sources, and nitrate removal change from upstream to downstream.

It would also be useful for future studies to investigate the EMMA hydrograph separation and nitrate mass balance over the course of individual storm events. Doing so would allow for a more detailed understanding of how water sources and nitrate sources behave on the rising and falling limbs of a storm hydrograph, and specifically whether water and nitrate sources behave in a coupled or decoupled manner throughout the storm. Such an investigation could yield insights into the nitrate flushing effect, in which nitrate concentrations peak before discharge peaks (Ocampo et al. 2006).

5.5.3. Management implications

From a management perspective, the finding that shallow groundwater has very high nitrate concentrations (Table 5) is concerning because over time this high-nitrate water may percolate downward into the Quaternary aquifer. The Quaternary aquifer is a common source of drinking water in the region (Bradt 1997), and high nitrate levels in Quaternary groundwater could force homeowners to drill deeper wells to access uncontaminated aquifers.

Furthermore, the result that shallow groundwater contributes significant amounts of water and nitrate to the stream demonstrates that water quality management should be influenced by the geology of the setting. For example, in two nearby watersheds in southern Minnesota, the Cobb River Watershed and the Blue Earth River Watershed, tile drainage composes approximately 90% of the stream discharge, and subsurface pathways are not a significant contributor to streamflow (Magner and Alexander 2002). This difference may be due to the more hummocky glacial landforms in these watersheds compared to the Cottonwood River Watershed (Jennings, Lusardi, and Gowan 2012; Gowan 2016b; Hobbs 2016); the irregular topography may impede subsurface water movement. Management of nitrate in these watersheds should take these differences in flow pathway into account. In the Cottonwood River Watershed steps should be taken to reduce nitrate infiltration into shallow groundater, while in the Cobb River and Blue Earth River Watersheds efforts should focus mainly on strategies to control nitrate loading from tile drains.

This study concluded that higher discharge levels will lead to increased nitrate export because less nitrate is removed from the stream biogeochemically at higher discharge levels. High nitrate exports from the Cottonwood River will contribute to nitrate contamination in the Minnesota River, the Mississippi River, and eventually to eutrophication in the Gulf of Mexico (Rabalais, Turner, and Wiseman 2002; Goolsby and Battaglin 2001). In order to minimize these effects, it will be important to take steps to reduce discharge levels in the Cottonwood River (Raymond, David, and Saiers 2012). Reduction of peak discharge and nitrate removal could be accomplished by restoring wetlands and riparian zones throughout the watershed (Mitsch et al. 2001).

6. Conclusion

This study investigated nitrate pathways and processes in the Cottonwood River Watershed, an agricultural landscape in southern Minnesota. Using an end-member mixing analysis, nitrate mass balance, and concentration-discharge analysis, the following conclusions were reached:

1. Streamflow in the Cottonwood River at Lamberton is principally composed of tile drainage, shallow groundwater, and deep (Quaternary aquifer) groundwater.
2. Nitrate is removed from the stream water via biogeochemical processes. Nitrate removal rates are highest at low discharges, which typically occur late in the crop growing season.
3. Concentration-discharge relationships corroborate biogeochemical removal of nitrate at low discharges. Additionally, concentration-discharge relationships provide evidence for more consistent nitrate concentrations throughout the year in the present than approximately 20 years ago, likely due to artificial drainage.

These findings highlight the importance of controlling nitrate concentrations in tile drainage, shallow groundwater, and deep groundwater, and of reducing peak flows in order to promote biogeochemical in-stream nitrate removal. This study also demonstrates the efficacy of combining an end-member mixing analysis based on short-term observations with analysis of long-term concentration-discharge data. Such an approach allowed this study to investigate specific pathways using the mixing analysis, as well as to demonstrate that these pathways are representative of the long-term nitrate dynamics in the watershed.

7. References

Alexander, Richard B., John Karl Böhlke, Elizabeth W. Boyer, Mark B. David, Judson W. Harvey, Patrick J. Mulholland, Sybil P. Seitzinger, Craig R. Tobias, Christina Tonitto, and Wilfred M. Wollheim. 2009. 'Dynamic modeling of nitrogen losses in river networks unravels the coupled effects of hydrological and biogeochemical processes', *Biogeochemistry*, 93: 91-116.

Alexander, Richard B., Richard A. Smith, and Gregory E. Schwarz. 2000. 'Effect of stream channel size on the delivery of nitrogen to the Gulf of Mexico', *Nature*, 403: 758-61.

Alexander, Scott. 2018. "Protocol for Water Sampling by MN DNR." In.

Ali, Geneviève A., André G. Roy, Marie-Claude Turmel, and François Courchesne. 2010. 'Source-to-stream connectivity assessment through end-member mixing analysis', *Journal of Hydrology*, 392: 119-35.

American Public Health Association, and Water Pollution Control Federation. 1960. *Standard methods for the examination of water and wastewater : including bottom sediments and sludges*.

Anderson, Kelsy A., and John A. Downing. 2006. 'Dry and wet atmospheric deposition of nitrogen, phosphorus and silicon in an agricultural region', *Water, Air, and Soil Pollution*, 176: 351-74.

Arnold, J.G., P.M. Allen, R. Muttiah, and G. Bernhardt. 1995. 'Automated base flow separation and recession analysis techniques', *Groundwater*, 33: 1010-18.

Asbjornsen, Heidi, German Mora, and Matthew J. Helmers. 2007. 'Variation in water uptake dynamics among contrasting agricultural and native plant communities in the Midwestern U.S', *Agriculture, Ecosystems & Environment*, 121: 343-56.

Barnes, B. S. 1940. 'Discussion of analysis of runoff characteristics', *Trans ASCE*: 105-06.

Basu, Nandita B., Georgia Destouni, James W. Jawitz, Sally E. Thompson, Natalia V. Loukinova, Amélie Darracq, Stefano Zanardo, Mary Yaeger, Murugesu Sivapalan, Andrea Rinaldo, and P. Suresh C. Rao. 2010. 'Nutrient loads exported from managed catchments reveal emergent biogeochemical stationarity', *Geophysical Research Letters*, 37: n/a-n/a.

Basu, Nandita B., Sally E. Thompson, and P. Suresh C. Rao. 2011. 'Hydrologic and biogeochemical functioning of intensively managed catchments: A synthesis of top-down analyses', *Water Resources Research*, 47.

Bernal, Susana, Andrea Butturini, and Francesc Sabater. 2006. 'Inferring nitrate sources through end member mixing analysis in an intermittent Mediterranean stream', *Biogeochemistry*, 81: 269-89.

Boano, F., A. Demaria, R. Revelli, and L. Ridolfi. 2010. 'Biogeochemical zonation due to intrameander hyporheic flow', *Water Resources Research*, 46.

Boerboom, Terrence J., Steenberg, Julia R. 2016. "Brown County Plate 2 - Bedrock Geology." In *County Atlas Series*. Minnesota Geological Survey.

Böhlke, J. K., J.W. Harvey, and Mary A. Voytek. 2004. 'Reach-scale isotope tracer experiment to quantify denitrification and related processes in a nitrate-rich stream, midcontinent United States', *Limnology and Oceanography*, 49: 821-38.

Bond, Nick. 2016. "Package 'hydrostats'." In. The Comprehensive R Archive Network (CRAN).
Booth, Mary S., and Chris Campbell. 2007. 'Spring Nitrate Flux in the Mississippi River Basin: A Landscape Model with Conservation Applications', *Environmental Science & Technology*, 41: 5410-18.
Bradt, Randy. 1997. "RHA-2, Part B, Plate 3 of 4: Surficial Hydrogeology." In *Regional Hydrogeologic Assessment Series*. Minnesota Department of Natural Resources, Division of Waters.
Briggs, Martin A., Laura K. Lautz, and Danielle K. Hare. 2014. 'Residence time control on hot moments of net nitrate production and uptake in the hyporheic zone', *Hydrological Processes*, 28: 3741-51.
Brooks, J. Renée, Parker J. Wigington, Donald L. Phillips, Randy Comeleo, and Rob Coulombe. 2012. 'Willamette River Basin surface water isoscape (δ18O and δ2H): temporal changes of source water within the river', *Ecosphere*, 3: art39.
Burgin, Amy J, and Stephen K Hamilton. 2007. 'Have we overemphasized the role of denitrification in aquatic ecosystems? A review of nitrate removal pathways', *Frontiers in Ecology and the Environment*, 5: 89-96.
Burns, Douglas A., Jeffrey J. McDonnell, Richard P. Hooper, Norman E. Peters, James E. Freer, Carol Kendall, and Keith Beven. 2001. 'Quantifying contributions to storm runoff through end-member mixing analysis and hydrologic measurements at the Panola Mountain Research Watershed (Georgia, USA)', *Hydrological Processes*, 15: 1903-24.
Christophersen, Nils, and Richard P. Hooper. 1992. 'Multivariate analysis of stream water chemical data: The use of principal components analysis for the end-member mixing problem', *Water Resources Research*, 28: 99-107.
"Cleaning of Equipment for Water Sampling." In. 2004. edited by U. S. Geological Survey. U.S. Geological Survey.
"Climate Data for Lamberton Southwest Research and Outreach Center." In. 2018. edited by National Weather Service. MN Department of Natural Resources: MN Department of Natural Resources.
"Climate Data for Tracy." In. 2018. edited by National Weather Service. MN Department of Natural Resources: MN Department of Natural Resources.
Corsi, S. R., L. A. De Cicco, M. A. Lutz, and R. M. Hirsch. 2015. 'River chloride trends in snow-affected urban watersheds: increasing concentrations outpace urban growth rate and are common among all seasons', *Sci Total Environ*, 508: 488-97.
"County Boundaries, Minnesota." In. 2013. translated and edited by MN Department of Natural Resources. Minnesota Geospatial Commons: Minnesota Geospatial Commons.
David, Mark B., Laurie E. Drinkwater, and Gregory F. McIsaac. 2010. 'Sources of Nitrate Yields in the Mississippi River Basin', *Journal of Environment Quality*, 39: 1657.
Delwiche, Constant C. 1970. 'The nitrogen cycle', *Scientific American*, 223: 136-47.
Dierauer, Jennifer, and Paul Whitfield. 2017. "Package 'FlowScreen'." In. The Comprehensive R Archive Network (CRAN).
Divers, M. T., E. M. Elliott, and D. J. Bain. 2014. 'Quantification of nitrate sources to an urban stream using dual nitrate isotopes', *Environ Sci Technol*, 48: 10580-7.

Doctor, Daniel H., E. Calvin Alexander, Metka Petrič, Janja Kogovšek, Janko Urbanc, Sonja Lojen, and Willibald Stichler. 2006. 'Quantification of karst aquifer discharge components during storm events through end-member mixing analysis using natural chemistry and stable isotopes as tracers', *Hydrogeology Journal*, 14: 1171-91.

Donner, Simon D., Christopher J. Kucharik, and Jonathan A. Foley. 2004. 'Impact of changing land use practices on nitrate export by the Mississippi River', *Global Biogeochemical Cycles*, 18: n/a-n/a.

Eckhardt, K. 2005. 'How to construct recursive digital filters for baseflow separation', *Hydrological Processes*, 19: 507-15.

———. 2012. 'Technical Note: Analytical sensitivity analysis of a two parameter recursive digital baseflow separation filter', *Hydrology and Earth System Sciences*, 16: 451-55.

Galloway, J. N., J. D. Aber, J. W. Erisman, S. P. Seitzinger, R. W. Howarth, E. B. Cowling, and B. J. Cosby. 2003. 'The nitrogen cascade.', *AIBS Bulletin*, 53: 341-56.

Godsey, Sarah E., James W. Kirchner, and David W. Clow. 2009. 'Concentration-discharge relationships reflect chemostatic characteristics of US catchments', *Hydrological Processes*, 23: 1844-64.

Gonzales, A.L., J. Nonner, J. Heijkers, and S. Uhlenbrook. 2009. 'Comparison of different base flow separation methods in a lowland catchment', *Hydrology and Earth System Sciences*, 13: 2055-68.

Goolsby, Donald A., and William A. Battaglin. 2001. 'Long-term changes in concentrations and flux of nitrogen in the Mississippi River Basin, USA', *Hydrological Processes*, 15: 1209-26.

Gowan, Angela S. 2016a. "Redwood County Plate 4 - Quaternary Stratigraphy." In *County Atlas Series*. Minnesota Geological Survey.

Gowan, Angela S.; Jennings, Carrie E. 2016b. "Redwood County Plate 3 - Surficial Geology." In *County Atlas Series*. Minnesota Geological Survey.

Gracz, Michael B., Mary F. Moffett, Donald I. Siegel, and Paul H. Glaser. 2015. 'Analyzing peatland discharge to streams in an Alaskan watershed: An integration of end-member mixing analysis and a water balance approach', *Journal of Hydrology*, 530: 667-76.

Green, C. T., B. A. Bekins, S. J. Kalkhoff, R. M. Hirsch, L. Liao, and K. K. Barnes. 2014. 'Decadal surface water quality trends under variable climate, land use, and hydrogeochemical setting in Iowa, USA.', *Water Resources Research*, 50: 2425-43.

Green, Mark B., John L. Nieber, Greg Johnson, Joe Magner, and Brennon Schaefer. 2007. 'Flow path influence on an N:P ratio in two headwater streams: A paired watershed study', *Journal of Geophysical Research: Biogeosciences*, 112: n/a-n/a.

'Ground Water and Drinking Water: National Primary Drinking Water Regulations'. U.S. Environmental Protection Agency, Accessed April 10, 2018. **https://www.epa.gov/ground-water-and-drinking-water/national-primary-drinking-water-regulations - Inorganic**.

Gruber, N., and J. N. Galloway. 2008. 'An Earth-system perspective of the global nitrogen cycle', *Nature*, 451: 293-6.
Gu, Chuanhui, George M. Hornberger, Aaron L. Mills, Janet S. Herman, and Samuel A. Flewelling. 2007. 'Nitrate reduction in streambed sediments: Effects of flow and biogeochemical kinetics', *Water Resources Research*, 43.
Hach. 2014. "Nitratax sc User Manual." In, 42.
Harvey, Judson W., J. K. Böhlke, Mary A. Voytek, Durelle Scott, and Craig R. Tobias. 2013. 'Hyporheic zone denitrification: Controls on effective reaction depth and contribution to whole-stream mass balance', *Water Resources Research*, 49: 6298-316.
Hill, A. R., C. F. Labadia, and K. Sanmugadas. 1998. 'Hyporheic zone hydrology and nitrogen dynamics in relation to the streambed topography of a N-rich stream', *Biogeochemistry*, 42: 285-310.
Hirsch, R.M., and L.A. De Cicco. 2015. 'User guide to Exploration and Graphics for RivEr Trends (EGRET) and dataRetrieval: R packages for hydrologic data', *U.S. Geological Survey Techniques and Methods*, Book 4, chapter A10: 93 p.
Hirsch, Robert M., Douglas L. Moyer, and Stacey A. Archfield. 2010. 'Weighted Regressions on Time, Discharge, and Season (WRTDS), with an Application to Chesapeake Bay River Inputs1', *JAWRA Journal of the American Water Resources Association*, 46: 857-80.
Hobbs, Howard C., Knaeble, Alan R. 2016. "Brown County Plate 3 - Surficial Geology." In *County Atlas Series*. Minnesota Geological Survey.
Hooper, Richard P. 2003. 'Diagnostic tools for mixing models of stream water chemistry', *Water Resources Research*, 39.
———. 2016. 'End Member Mixing Analysis spreadsheet.'. **http://www.hydroshare.org/resource/9ad1ebc69e9a4eda948ecd33155aae4c**.
Inamdar, Shreeram. 2011. 'The Use of Geochemical Mixing Models to Derive Runoff Sources and Hydrologic Flow Paths.' in D. F. Levia, D. Carlyle-Moses and T. Tanaka (eds.), *Forest hydrology and biogeochemistry: synthesis of past research and future directions.* (Springer Science & Business Media).
Inamdar, Shreeram, Gurbir Dhillon, Shatrughan Singh, Sudarshan Dutta, Delphis Levia, Durelle Scott, Myron Mitchell, John Van Stan, and Patrick McHale. 2013. 'Temporal variation in end-member chemistry and its influence on runoff mixing patterns in a forested, Piedmont catchment', *Water Resources Research*, 49: 1828-44.
Inamdar, Shreeram P., and Myron J. Mitchell. 2007. 'Contributions of riparian and hillslope waters to storm runoff across multiple catchments and storm events in a glaciated forested watershed', *Journal of Hydrology*, 341: 116-30.
James, April L., and Nigel T. Roulet. 2006. 'Investigating the applicability of end-member mixing analysis (EMMA) across scale: A study of eight small, nested catchments in a temperate forested watershed', *Water Resources Research*, 42.
Jennings, Carrie E., Barbara A. Lusardi, and Angela S. Gowan. 2012. "Blue Earth County Plate 3 - Surficial Geology." In *County Atlas Series*. Minnesota Geological Survey.

Jirsa, Mark A., Chandler, V.W., Setterholm, Dale R. 2016. "Redwood County Plate 2 - Bedrock Geology." In *County Atlas Series*. Minnesota Geological Survey.
Jung, Helen Y., Terri S. Hogue, Laura K. Rademacher, and Tom Meixner. 2009. 'Impact of wildfire on source water contributions in Devil Creek, CA: evidence from end-member mixing analysis', *Hydrological Processes*, 23: 183-200.
Kelly, Valerie, Edward G. Stets, and Charlie Crawford. 2015. 'Long-term changes in nitrate conditions over the 20th century in two Midwestern Corn Belt streams', *Journal of Hydrology*, 525: 559-71.
Kessler, Erich. 2018. "Methods for Stream Gage at Cottonwood River nr New Ulm Site 05317000." In.
King, K. W., N. R. Fausey, and M. R. Williams. 2014. 'Effect of subsurface drainage on streamflow in an agricultural headwater watershed', *Journal of Hydrology*, 519: 438-45.
Klaus, J., and J. J. McDonnell. 2013. 'Hydrograph separation using stable isotopes: Review and evaluation', *Journal of Hydrology*, 505: 47-64.
Knaeble, Alan R. 2016. "Brown County Plate 4 - Quaternary Stratigraphy." In *County Atlas Series*. Minnesota Geological Survey.
Kreiling, R. M., and J. N. Houser. 2016. 'Long-term decreases in phosphorus and suspended solids, but not nitrogen, in six upper Mississippi River tributaries, 1991-2014', *Environ Monit Assess*, 188: 454.
Ladson, A. R., R. Brown, B. Neal, and R. Nathan. 2013. 'A standard approach to baseflow separation using the Lyne and Hollick filter', *Australian Journal of Water Resources*, 17.
Lee, Douglas H. K. 1970. 'Nitrates, Nitrites, and Methemoglobinemia', *Environmental Research*, 3: 484-511.
Lenhart, C. F., E. S. Verry, K. N. Brooks, and J. A. Magner. 2012. 'Adjustment of Prairie Pothole Streams to Land-Use, Drainage and Climate Changes and Consequences for Turbidity Impairment', *River Research and Applications*, 28: 1609-19.
Linsley Jr., Ray K., Max A. Kohler, and Joseph L. H. Paulhus. 1958. *Hydrology for Engineers* (McGraw-Hill Book Company).
Liu, Fengjing, Martha H. Conklin, and Glenn D. Shaw. 2017. 'Insights into hydrologic and hydrochemical processes based on concentration-discharge and end-member mixing analyses in the mid-Merced River Basin, Sierra Nevada, California', *Water Resources Research*, 53: 832-50.
Lyne, V., and M. Hollick. 1979. "Stochastic Time-Variable Rainfall-Runoff Modelling." In *Institute of Engineers Australia National Conference*, 89-93.
Magner, J. A., G. A. Payne, and L. J. Steffen. 2004. 'Drainage effects on stream nitrate-N and hydrology in south-central Minnesota (USA).', *Environmental monitoring and assessment*, 91: 183-98.
Magner, J.A., and S.C. Alexander. 2002. 'Geochemical and isotopic tracing of water in nested southern Minnesota corn-belt watersheds.', *Water Science and Technology*, 45.
Matson, P., K. A. Lohse, and S. J. Hall. 2002. 'The globalization of nitrogen deposition: consequences for terrestrial ecosystems.', *AMBIO: A Journal of the Human Environment,*, 31: 113-19.

Maurya, A. S., Miral Shah, R. D. Deshpande, R. M. Bhardwaj, A. Prasad, and S. K. Gupta. 2011. 'Hydrograph separation and precipitation source identification using stable water isotopes and conductivity: River Ganga at Himalayan foothills', *Hydrological Processes*, 25: 1521-30.

"Minnesota Digital Elevation Model - 30 Meter Resolution." In. 2018. edited by U.S. Geological Survey. Minnesota Geospatial Commons: Minnesota Geospatial Commons.

"Minnesota River - Cottonwood River Watershed." In., edited by Minnesota Pollution Control Agency.

"Minnesota Well Index." In., edited by MN Department of Health. MN Department of Health.

Mitsch, W. J., J. W. Day Jr, J. W. Gilliam, P. M. Groffman, D. L. Hey, G. W. Randall, and N. Wang. 2001. 'Reducing Nitrogen Loading to the Gulf of Mexico from the Mississippi River Basin: Strategies to Counter a Persistent Ecological Problem', *BioScience*, 51: 373-88.

"MN Department of Natural Resources: Water Chemistry Data." In. 2017. edited by MN Department of Natural Resources. MN Department of Natural Resources.

MNDNR. 2014. "Cottonwood River nr Lamberton, US14." In.: MN DNR.

"MNDNR Hydrography." In. 2018. edited by MN Department of Natural Resources. Minnesota Geospatial Commons: Minnesota Geospatial Commons.

"MNDNR Watershed Suite." In. 2018. edited by MN Department of Natural Resources. Minnesota Geospatial Commons: Minnesota Geospatial Commons.

Moatar, F., B. W. Abbott, C. Minaudo, F. Curie, and G. Pinay. 2017. 'Elemental properties, hydrology, and biology interact to shape concentration-discharge curves for carbon, nutrients, sediment, and major ions', *Water Resources Research*, 53: 1270-87.

Mulholland, P. J., A. M. Helton, G. C. Poole, R. O. Hall, S. K. Hamilton, B. J. Peterson, J. L. Tank, L. R. Ashkenas, L. W. Cooper, C. N. Dahm, W. K. Dodds, S. E. Findlay, S. V. Gregory, N. B. Grimm, S. L. Johnson, W. H. McDowell, J. L. Meyer, H. M. Valett, J. R. Webster, C. P. Arango, J. J. Beaulieu, M. J. Bernot, A. J. Burgin, C. L. Crenshaw, L. T. Johnson, B. R. Niederlehner, J. M. O'Brien, J. D. Potter, R. W. Sheibley, D. J. Sobota, and S. M. Thomas. 2008. 'Stream denitrification across biomes and its response to anthropogenic nitrate loading', *Nature*, 452: 202-5.

Nathan, R.J., and T.A McMahon. 1990. 'Evaluation of Automated Techniques for Base Flow and Recession Analyses', *Water Resources Research*, 26: 1465-73.

"National Atmospheric Deposition Program: National Trends Network, Lamberton, MN." In. 2017. edited by National Atmospheric Deposition Program.

Novotny, Eric V., and Heinz G. Stefan. 2007. 'Stream flow in Minnesota: Indicator of climate change', *Journal of Hydrology*, 334: 319-33.

Ocampo, Carlos J., Carolyn E. Oldham, Murugesu Sivapalan, and Jeffrey V. Turner. 2006. 'Hydrological versus biogeochemical controls on catchment nitrate export: a test of the flushing mechanism', *Hydrological Processes*, 20: 4269-86.

Patterson, Carrie J. 1997. 'Southern Laurentide ice lobes were created by ice streams: Des Moines Lobe in Minnesota, USA', *Sedimentary Geology*, 111: 249-61.

Pellerin, B. A., B. A. Bergamaschi, R. J. Gilliom, C. G. Crawford, J. Saraceno, C. P. Frederick, B. D. Downing, and J. C. Murphy. 2014. 'Mississippi River nitrate loads from high frequency sensor measurements and regression-based load estimation', *Environ Sci Technol*, 48: 12612-9.

Peterson, B. J., Wilfred M. Wollheim, P. J. Mulholland, J. R. Webster, J. L. Meyer, J. L. Tank, E. Martí, W. B. Bowden, H. M. Valett, A. E. Hershey, W. H. McDowell, W. K. Dodds, S. K. Hamilton, S. Gregory, and D. D. Morrall. 2001. 'Control of Nitrogen Export from Watersheds by Headwater Streams', *Science*, 292: 86-90.

Piña-Ochoa, E., and M. Álvarez-Cobelas. 2006. 'Denitrification in Aquatic Environments: A Cross-system Analysis', *Biogeochemistry*, 81: 111-30.

Potter, Kenneth W., Jamie C. Douglas, and Edmund M. Brick. 2004. 'Impacts of agriculture on aquatic ecosystems in the humid United States', 153: 31-39.

Puckett, L. J. 2004. 'Hydrogeologic controls on the transport and fate of nitrate in ground water beneath riparian buffer zones: results from thirteen studies across the United States', *Water Science and Technology*, 49: 47-53.

"R: A Language and Environment for Statistical Computing." In. 2017. edited by R Core Team. The R Foundation for Statistical Computing.

Rabalais, Nancy N., R. Eugene Turner, and William J. Wiseman. 2002. 'Gulf of Mexico Hypoxia, A.K.A. "The Dead Zone"', *Annual Review of Ecology and Systematics*, 33: 235-63.

Ranaivoson, Andry. 2018. "Tile drainage nitrate data." In.

Ranalli, Anthony J., and Donald L. Macalady. 2010. 'The importance of the riparian zone and in-stream processes in nitrate attenuation in undisturbed and agricultural watersheds – A review of the scientific literature', *Journal of Hydrology*, 389: 406-15.

"Rapid Watershed Assessment Resource Profile: Cottonwood (MN) HUC: 7020008." In., edited by U.S. Department of Agriculture: Natural Resources Conservation Service.

Raymond, Peter A., Mark B. David, and James E. Saiers. 2012. 'The impact of fertilization and hydrology on nitrate fluxes from Mississippi watersheds', *Current Opinion in Environmental Sustainability*, 4: 212-18.

Rutledge, A.T. 1998. "Computer Programs for Describing the Recession of Ground-Water Discharge and for Estimating Mean Ground-Water Recharge and Discharge from Streamflow Records—Update." In, edited by U.S. Geological Survey. Reston, Virginia.

Rütting, T., P. Boeckx, C. Müller, and L. Klemedtsson. 2011. 'Assessment of the importance of dissimilatory nitrate reduction to ammonium for the terrestrial nitrogen cycle', *Biogeosciences*, 8: 1779-91.

Schilling, K. E., E. McLellan, and E. A. Bettis, 3rd. 2013. 'Letting wet spots be wet: restoring natural bioreactors in the dissected glacial landscape', *Environ Manage*, 52: 1440-52.

Schilling, Keith E., and Matthew Helmers. 2008. 'Effects of subsurface drainage tiles on streamflow in Iowa agricultural watersheds: Exploratory hydrograph analysis', *Hydrological Processes*, 22: 4497-506.

Schilling, Keith E., Priyanka Jindal, Nandita B. Basu, and Matthew J. Helmers. 2012. 'Impact of artificial subsurface drainage on groundwater travel times and baseflow discharge in an agricultural watershed, Iowa (USA)', *Hydrological Processes*, 26: 3092-100.

Schottler, Shawn P., Jason Ulrich, Patrick Belmont, Richard Moore, J. Wesley Lauer, Daniel R. Engstrom, and James E. Almendinger. 2014. 'Twentieth century agricultural drainage creates more erosive rivers', *Hydrological Processes*, 28: 1951-61.

Seitzinger, Sybil, John A Harrison, JK Böhlke, AF Bouwman, Robert Lowrance, Bruce Peterson, C Tobias, and G Van Drecht. 2006. 'Denitrification across landscapes and waterscapes: a synthesis', *Ecological Applications*, 16: 2064-90.

Sklash, Michael G., and Robert N. Farvolden. 1979. 'The role of groundwater in storm runoff', *Journal of Hydrology*, 43: 45-65.

Sprague, L. A., R. M. Hirsch, and B. T. Aulenbach. 2011. 'Nitrate in the Mississippi River and its tributaries, 1980 to 2008: are we making progress?', *Environ Sci Technol*, 45: 7209-16.

"Tile Monitoring Project: Tile Reinventory." In.: Minnesota State University Water Resources Center.

Tomer, Mark D., and Keith E. Schilling. 2009. 'A simple approach to distinguish land-use and climate-change effects on watershed hydrology', *Journal of Hydrology*, 376: 24-33.

University of Minnesota: Southwest Research and Outreach Station - Lamberton, MN. 2018. 'Weather', Accessed Friday, March 9, 2017. **https://swroc.cfans.umn.edu/weather/precip-graphs**.

Valett, H. M., J. A. Morrice, and C. N. Dahm. 1996. 'Parent lithology, surface-groundwater exchange, and nitrate retention in headwater streams', *Limnology and Oceanography*, 41: 333-45.

van Verseveld, Willem J., Jeffrey J. McDonnell, and Kate Lajtha. 2008. 'A mechanistic assessment of nutrient flushing at the catchment scale', *Journal of Hydrology*, 358: 268-87.

Vitousek, P.M., J.D. Aber, R.W. Howarth, G.E. Likens, P.A. Matson, D.W. Schindler, W.H. Schlesinger, and D.G. Tilman. 1997. 'Human alteration of the global nitrogen cycle: sources and consequences', *Ecological Applications*, 7: 737-50.

"Water-Table Elevation and Depth to Water Table, Minnesota Hydrogeology Atlas series HG-03." In. 2016. edited by MN Department of Natural Resources. Minnesota Geospatial Commons: Minnesota Geospatial Commons.

"Watershed Context Report: Cottonwood River." In. 2017. edited by Minnesota Department of Natural Resources.

YSI. 2012. "6-Series Multiparameter Water Quality Sondes User Manual." In.

Zarnetske, Jay P., Roy Haggerty, Steven M. Wondzell, and Michelle A. Baker. 2011. 'Dynamics of nitrate production and removal as a function of residence time in the hyporheic zone', *Journal of Geophysical Research*, 116.

Zarnetske, Jay P., Roy Haggerty, Steven M. Wondzell, Vrushali A. Bokil, and Ricardo González-Pinzón. 2012. 'Coupled transport and reaction kinetics control the nitrate source-sink function of hyporheic zones', *Water Resources Research*, 48.

Zhang, Ruigang, Qiang Li, Thien Lien Chow, Sheng Li, and Serban Danielescu. 2013. 'Baseflow separation in a small watershed in New Brunswick, Canada, using a recursive digital filter calibrated with the conductivity mass balance method', *Hydrological Processes*, 27: 2659-65.

8. Appendix

Table A-1. Results from comparison of Nitratax determination of NO_{2+3}^--N (mg/L) and ion chromatograph determination of NO_{2+3}^--N (mg/L) from samples collected on May 30, 2017. Differences between the two methods lie within the Nitratax margin of error.

Sample ID	Nitratax NO_{2+3}^--N (mg/L)	Nitratax margin of error (mg/L)	IC NO_{2+3}^--N (mg/L)	Difference between Nitratax and IC (mg/L)
9HS	10.15	0.65	9.63	0.52
11HR	0.20	0.50	0.32	0.12
14PD	23.63	0.85	23.17	0.46
15PS	10.57	0.66	10.19	0.38
16PR	0.03	0.50	0.06	0.02
19WR	0.30	0.50	0.12	0.18

Table A-2. Cation, nitrate plus nitrite, and conductivity data from field blank. Nitrate plus nitrate was measured with the Nitratax probe. Conductivity was measured with the YSI sonde.

Ca (mg/L)	Mg (mg/L)	Na (mg/L)	Si (mg/L)	NO_{2+3}^--N (mg/L)	Conductivity (mS/cm)
0.908	0.190	0.066	0.209	0.0	0.012

Table A-3. Linear relationships between Lamberton and New Ulm discharge, winter season.

Time Period	Number of data points	Equation (y = Lamberton discharge, m3/s; x = New Ulm discharge, m3/s)	R^2 Value
November 20 – December 31	183	y = 0.2803 x + 1.2506	0.7569
January 1 – Feburary 28	185	y = 0.4045 x + 1.2703	0.7289
March 1 – April 10	333	y = 0.3184 x + 1.5324	0.87

Table A-4. Results from WRTDS sensitivity analysis.

WRTDS Sensitivity Analysis Results Nitrate Concentration, April through October			
Year	**Complete year of discharge and nitrate concentration data used NO_3^- (mg/L)**	**Dec., Jan., & Feb. discharge set at 0.0028 m^3/s; Dec., Jan., & Feb. nitrate data removed NO_3^- (mg/L)**	**Absolute value of difference between model runs NO_3^- (mg/L)**
1997	4.25	4.16	0.09
1998	2.98	2.92	0.06
1999	3.65	3.50	0.15
2000	2.04	1.99	0.05
2001	4.97	4.98	0.01
2002	5.34	5.15	0.19
2003	3.71	3.60	0.11
2004	5.18	5.13	0.05
2005	6.89	6.78	0.11
2006	5.95	5.90	0.05
2007	5.54	5.35	0.19
2008	5.03	4.88	0.15
2009	2.31	2.21	0.10
2010	8.13	7.94	0.19
2011	6.94	6.84	0.10
2012	3.10	3.07	0.03
2013	3.54	3.53	0.01
2014	4.26	4.26	0.00
2015	4.01	4.06	0.05
2016	10.23	10.05	0.18
2017	8.28	8.20	0.08

Table A-5. Interquartile ranges for EMMA end-member contributions to streamflow.

Sample Information		**End-Member Percentages to Streamflow, with Interquartile Ranges**					
Date	Discharge (m^3/s)	Tile		Spring		Quaternary Groundwater	
		Estimate	IQR	Estimate	IQR	Estimate	IQR
5/30/17	25.31	56.72%	0.00% to 80.17%	24.41%	0.00% to 74.90%	18.87%	15.13% to 61.39%
6/13/17	18.08	61.53%	0.00% to 81.84%	20.93%	0.00% to 75.41%	17.54%	13.97% to 57.41%
6/27/17	8.34	62.33%	0.00% to 80.96%	19.04%	0.00% to 74.27%	18.62%	14.91% to 60.69%
7/11/17	3.64	41.58%	0.00% to 80.45%	42.02%	0.00% to 79.55%	16.40%	13.02% to 53.79%
7/24/17	8.15	61.61%	25.05% to 86.11%	29.90%	3.77% to 62.53%	8.49%	6.11% to 30.00%
9/17/17	1.89	10.84%	0.00% to 46.58%	75.54%	36.77% to 86.89%	13.62%	10.66% to 39.05%